

Supporting Information

Breaking Thiocalixarene into Pieces – A Novel Synthetic Approach to Higher Calixarenes Bearing Mixed (-S-, -CH₂-) Bridges

Lukáš Kaiser,^a Tomáš Landovský,^a Karolína Salvadori,^b Václav Eigner,^c Hana Dvořáková^d and Pavel Lhoták^{a*}

^{a)} Department of Organic Chemistry, University of Chemistry and Technology, Prague (UCTP), Technická 5, 166 28 Prague 6, Czech Republic.

^{b)} Department of Physical Chemistry, UCTP, 166 28 Prague 6, Czech Republic.

^{c)} Department of Solid State Chemistry, UCTP, 166 28 Prague 6, Czech Republic.

^{d)} Laboratory of NMR spectroscopy, UCTP, 166 28 Prague 6, Czech Republic.

Table of Content

1. Spectral characterization of compounds	2
2. Fullerene complexation experiments	28
3. Crystallographic data	32
4. Reference	35

1. Spectral characterization of compounds

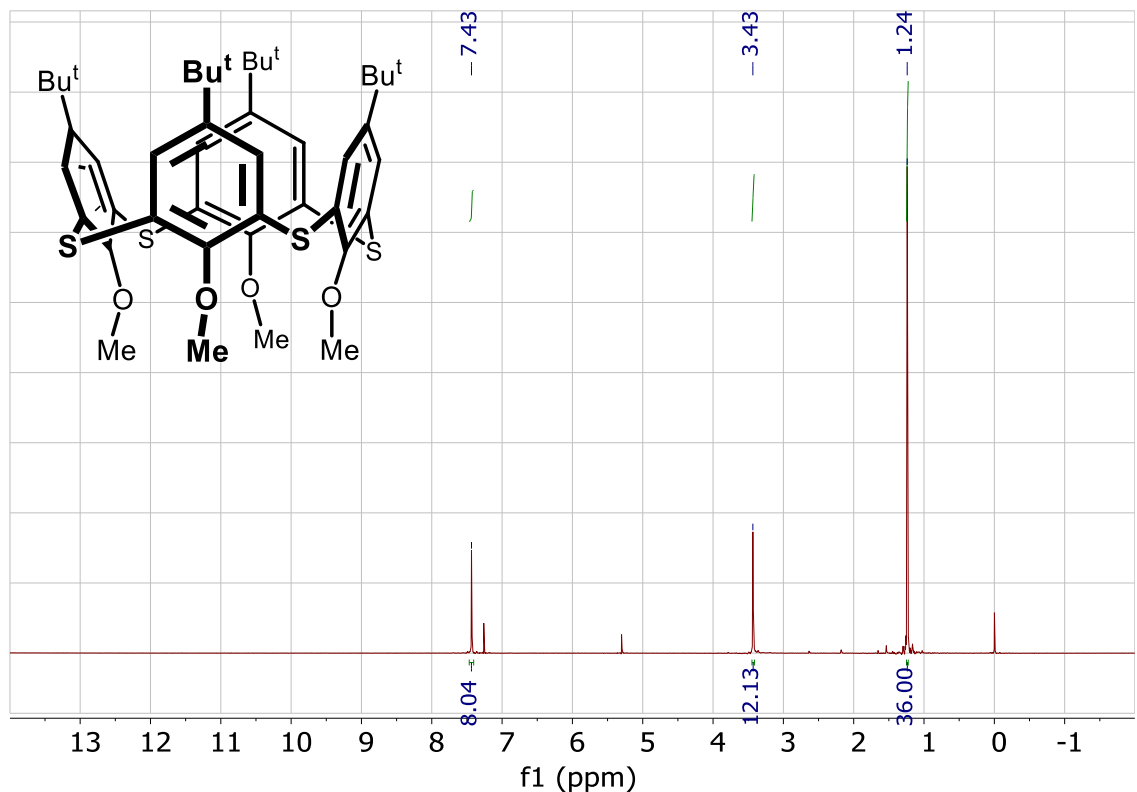


Figure 1. ¹H NMR spectrum of compound 2 (CDCl₃, 300 MHz)

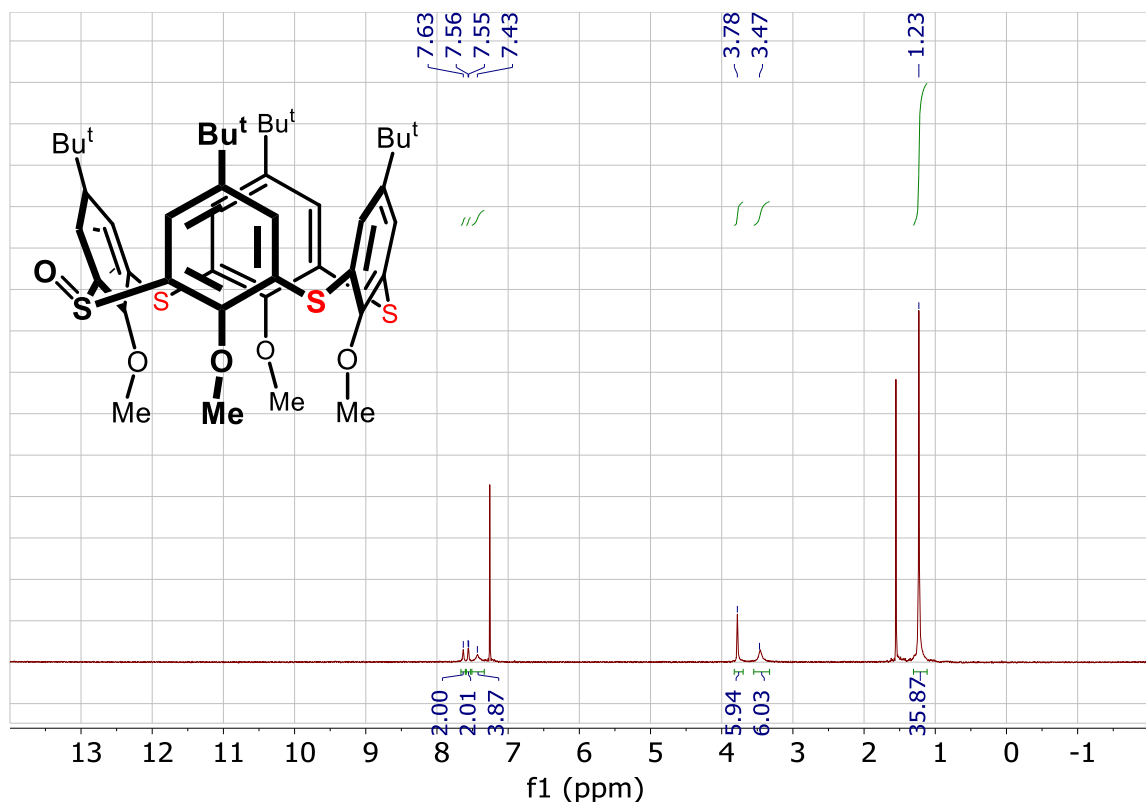


Figure 2. ¹H NMR spectrum of Compound 3 (CDCl₃, 300 MHz)

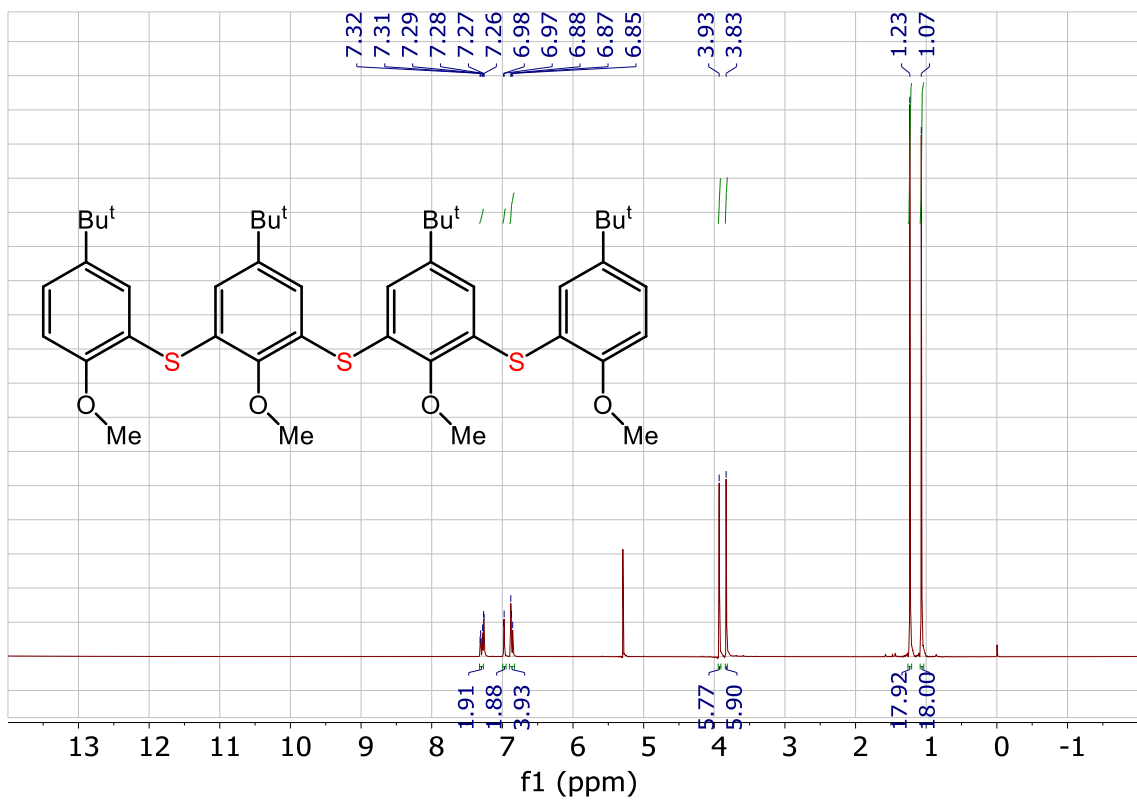


Figure 3. ^1H NMR spectrum of compound 4 (CDCl_3 , 300 MHz)

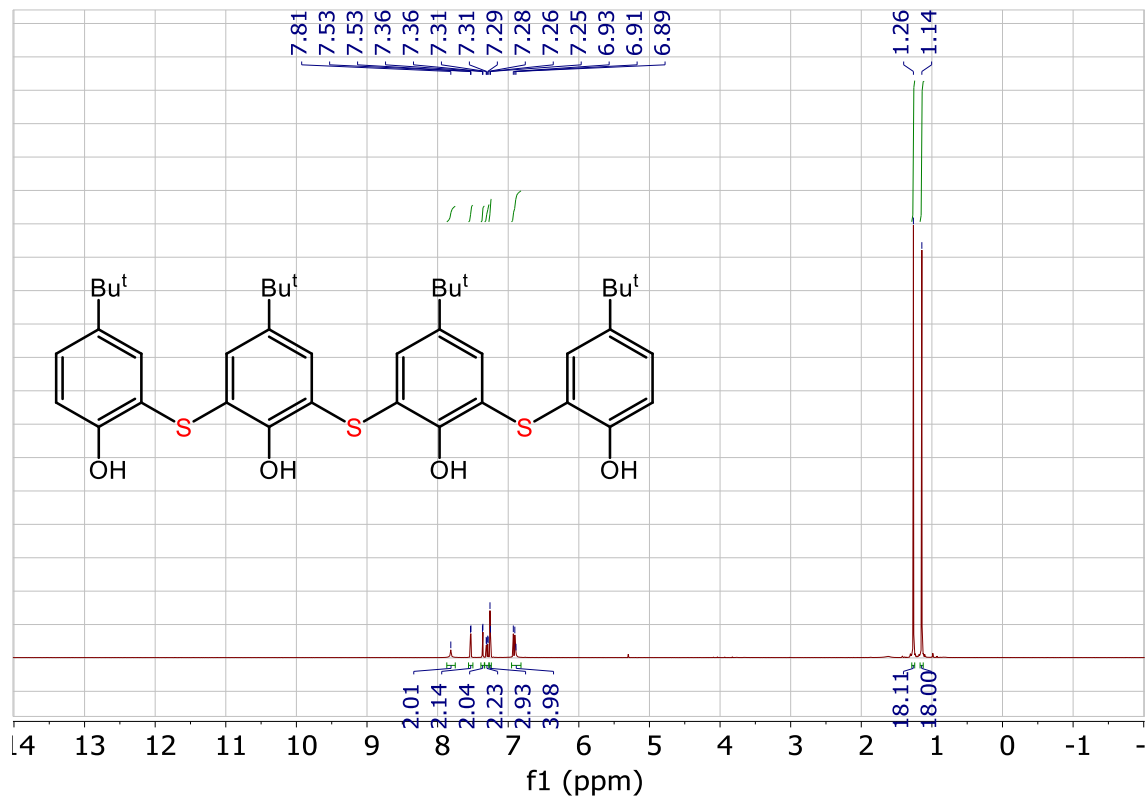


Figure 4. ^1H NMR spectrum of compound 5 (CDCl_3 , 300 MHz)

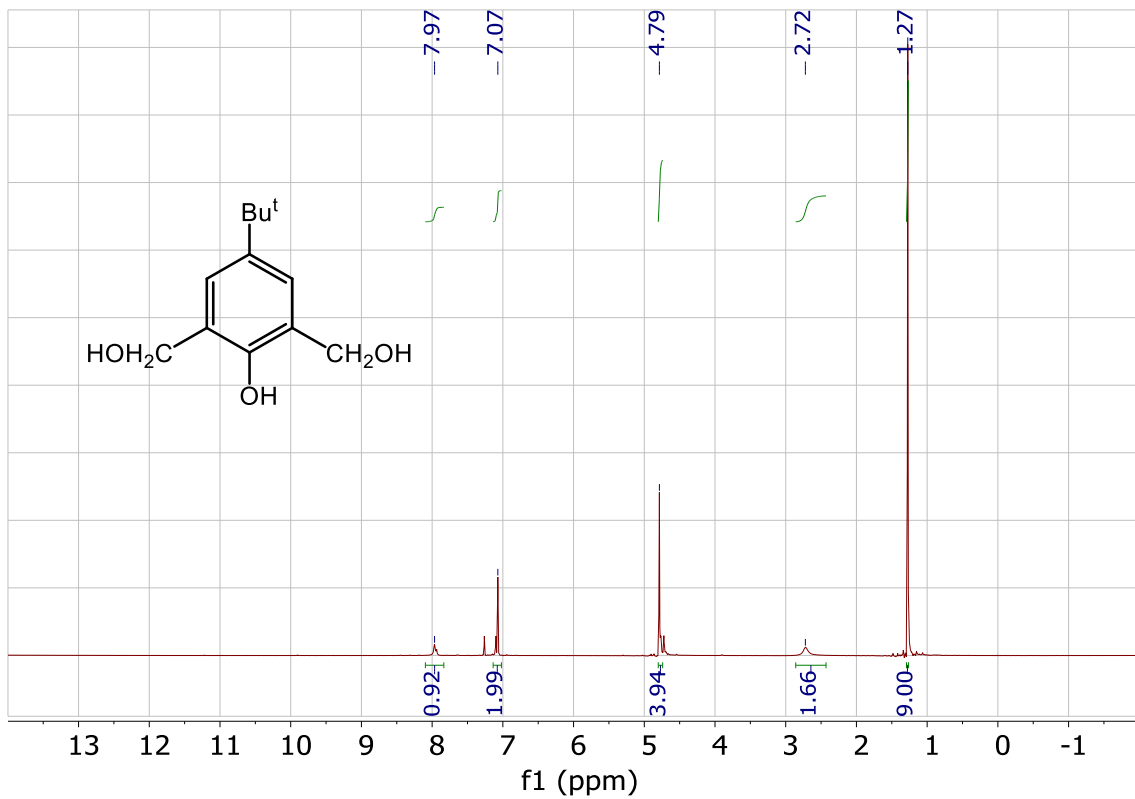


Figure 5. ^1H NMR spectrum of compound **6** (CDCl_3 , 300 MHz)

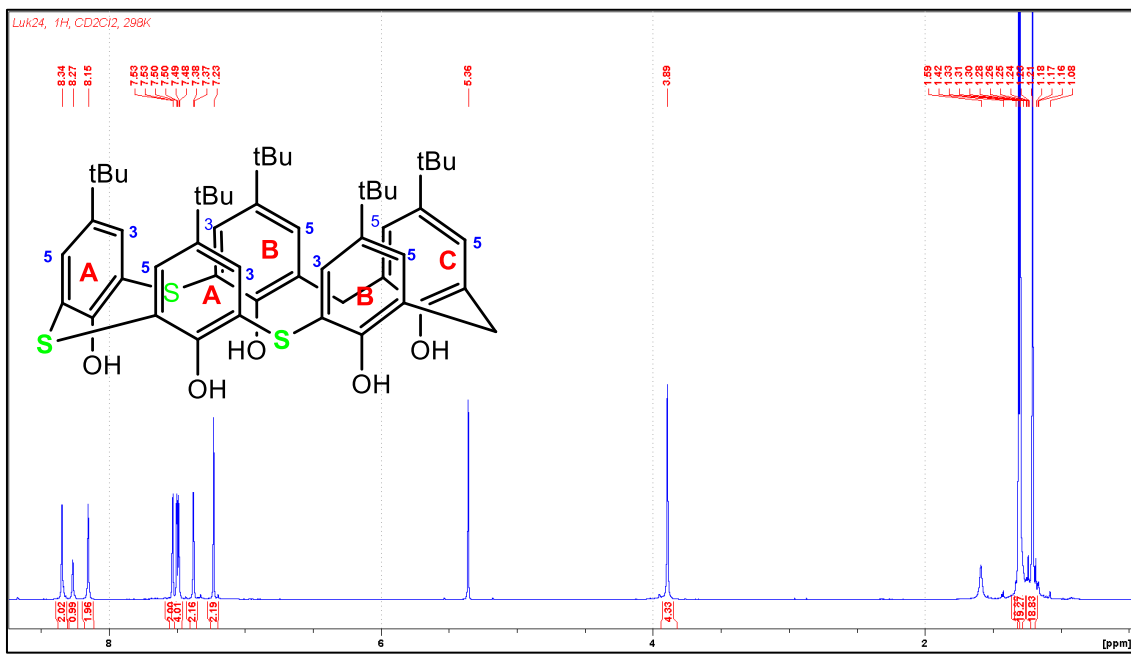


Figure 6. ^1H NMR spectrum of compound **8** (CD_2Cl_2 , 600 MHz)

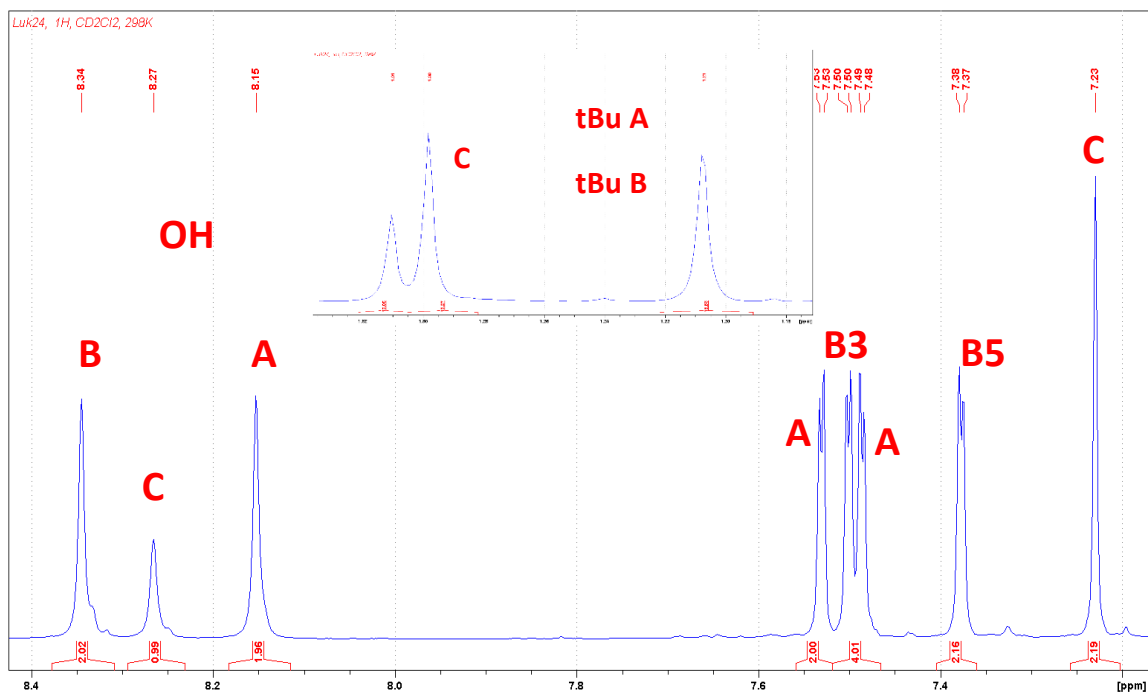


Figure 7. Assignment of ¹H NMR signals of compound **8** (CD₂Cl₂, 600 MHz)

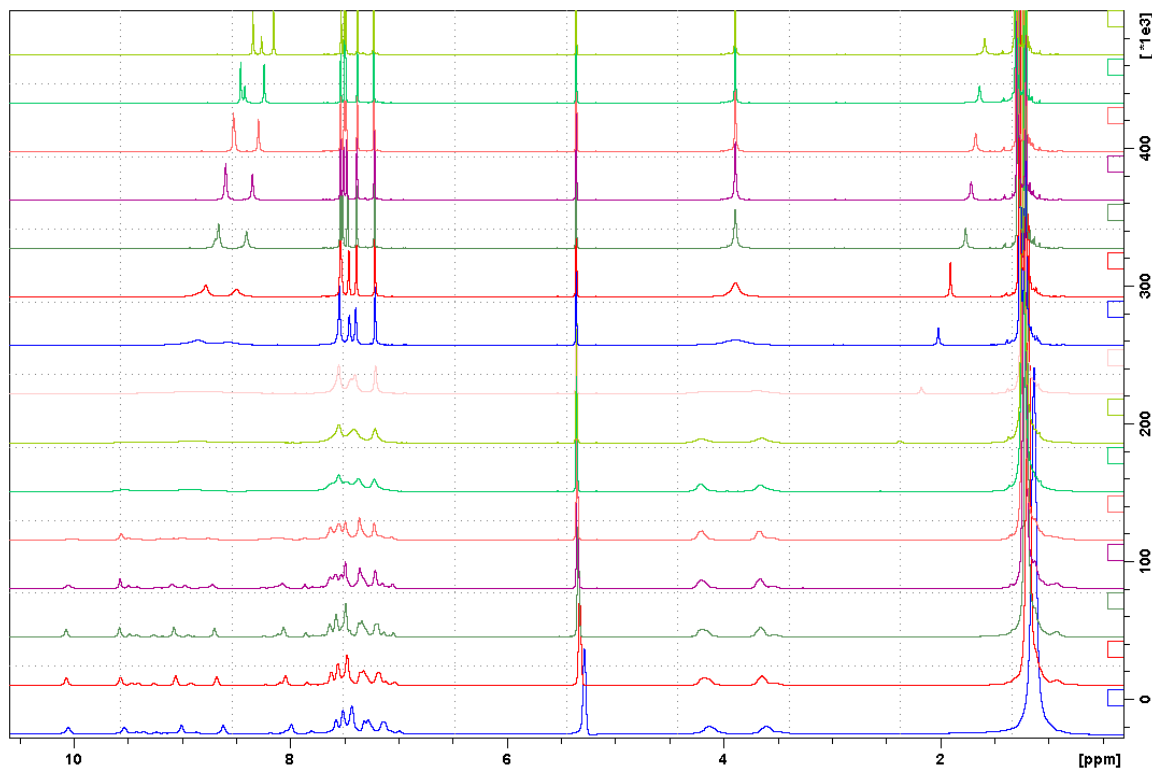


Figure 8. Variable temperature ¹H NMR experiments of compound **8** (298 – 153 K)

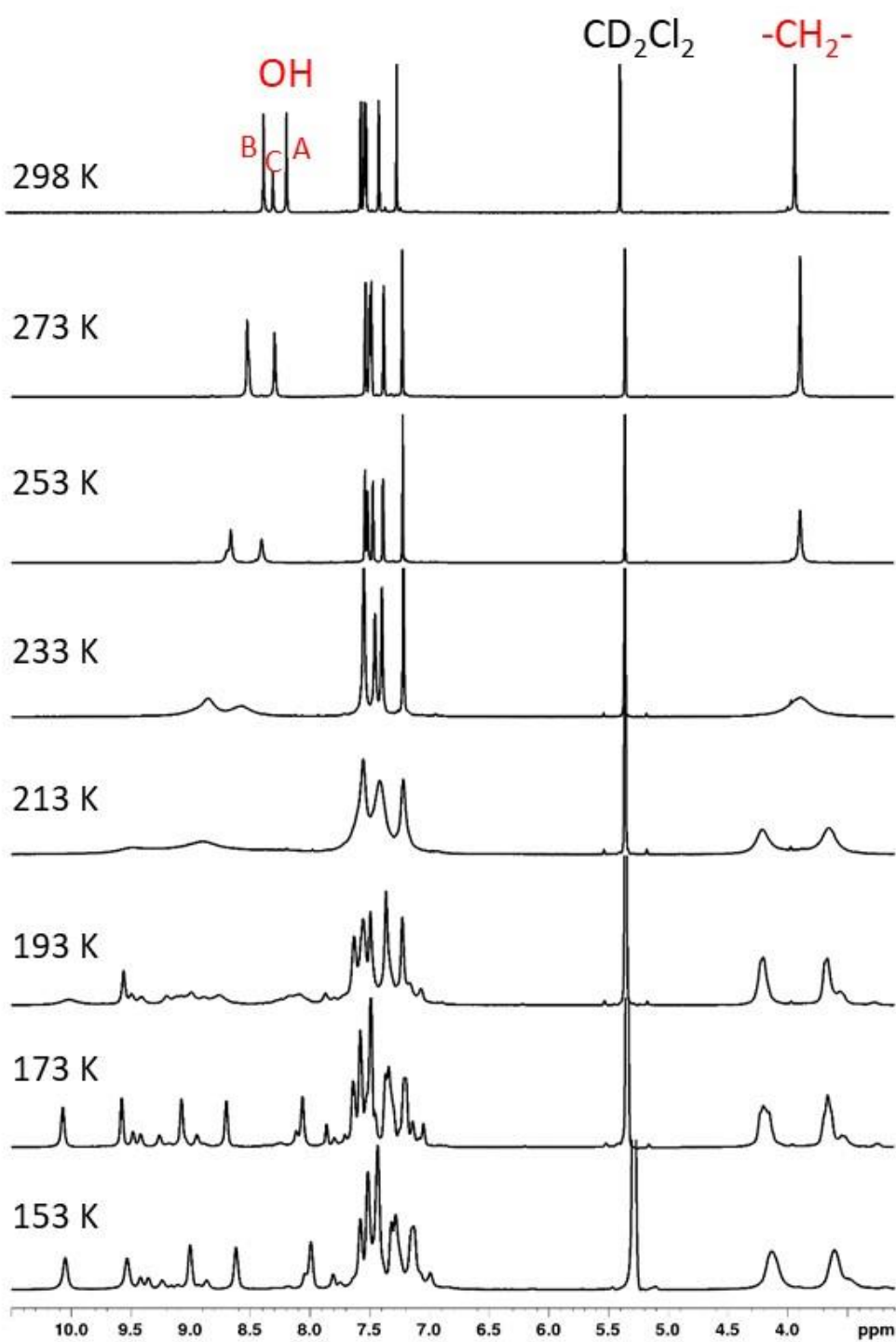


Figure 8a. The partial ¹H NMR spectra of **8** (phenolic OH and CH_2 area) at various temperatures (CD_2Cl_2 , 500 MHz) reflecting the *cone-cone* interconversion and the flip-flop motion of the circular HB array on the lower rim of calixarene.

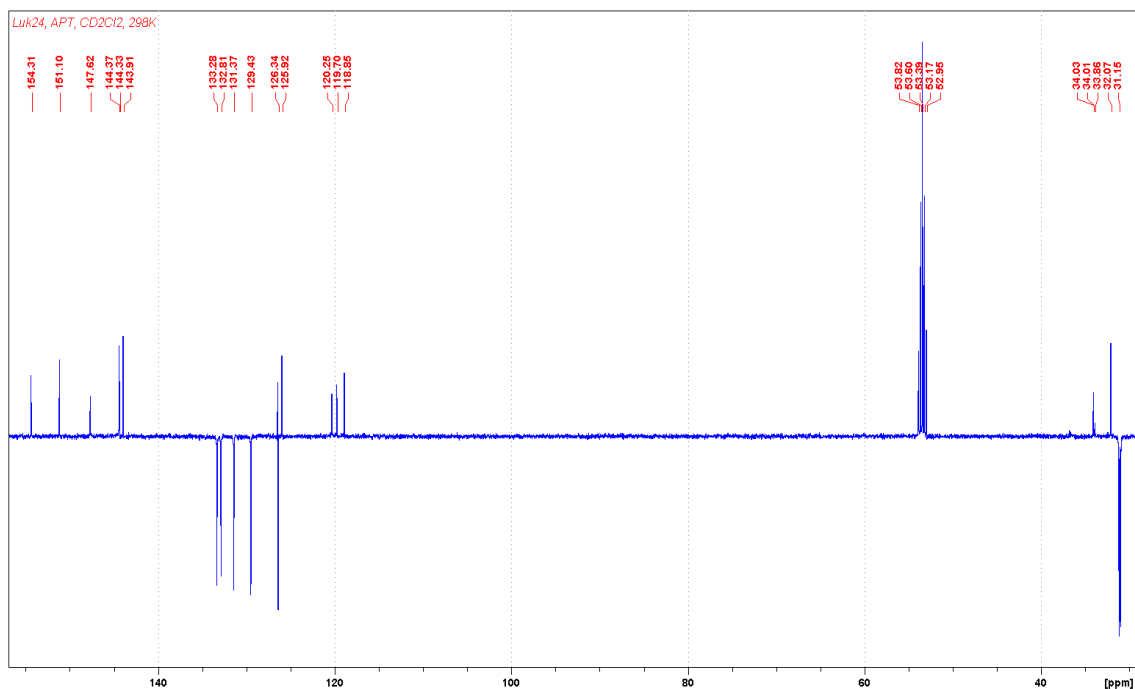


Figure 9. ¹³C NMR spectrum of compound **8** (CD₂Cl₂, 151 MHz)

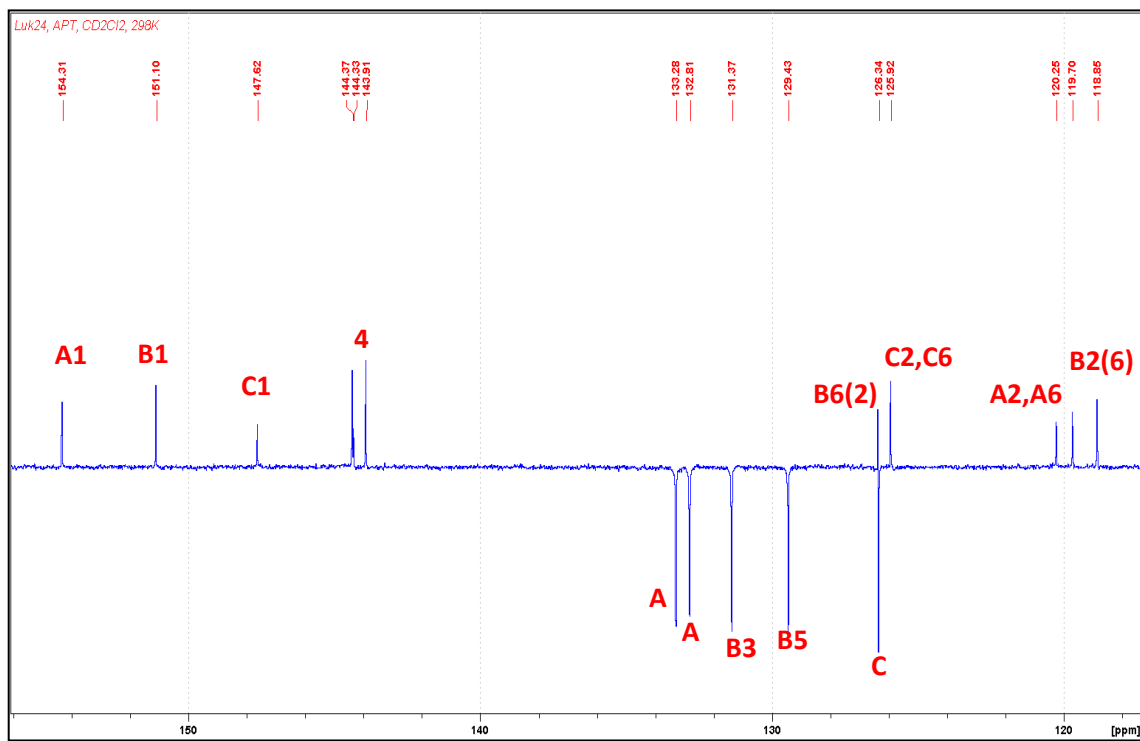


Figure 10. Assignment of ¹³C NMR signals of compound **8** (CD₂Cl₂, 151 MHz)

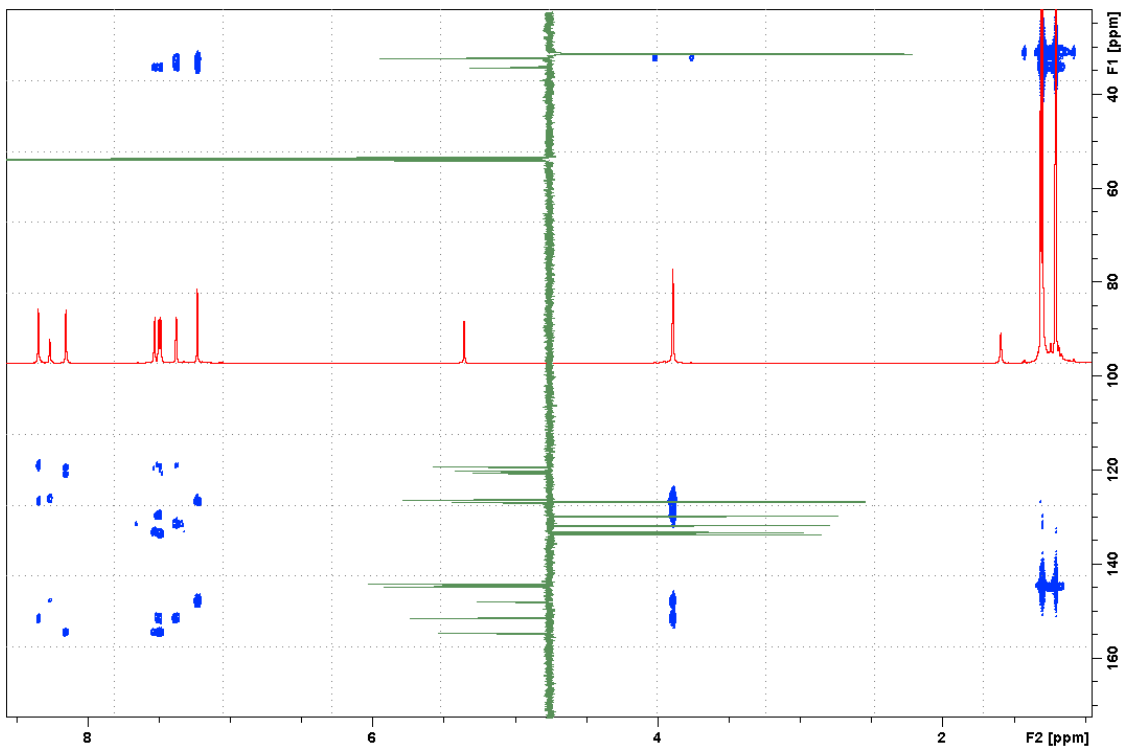


Figure 11. HMBC spectrum of compound 8

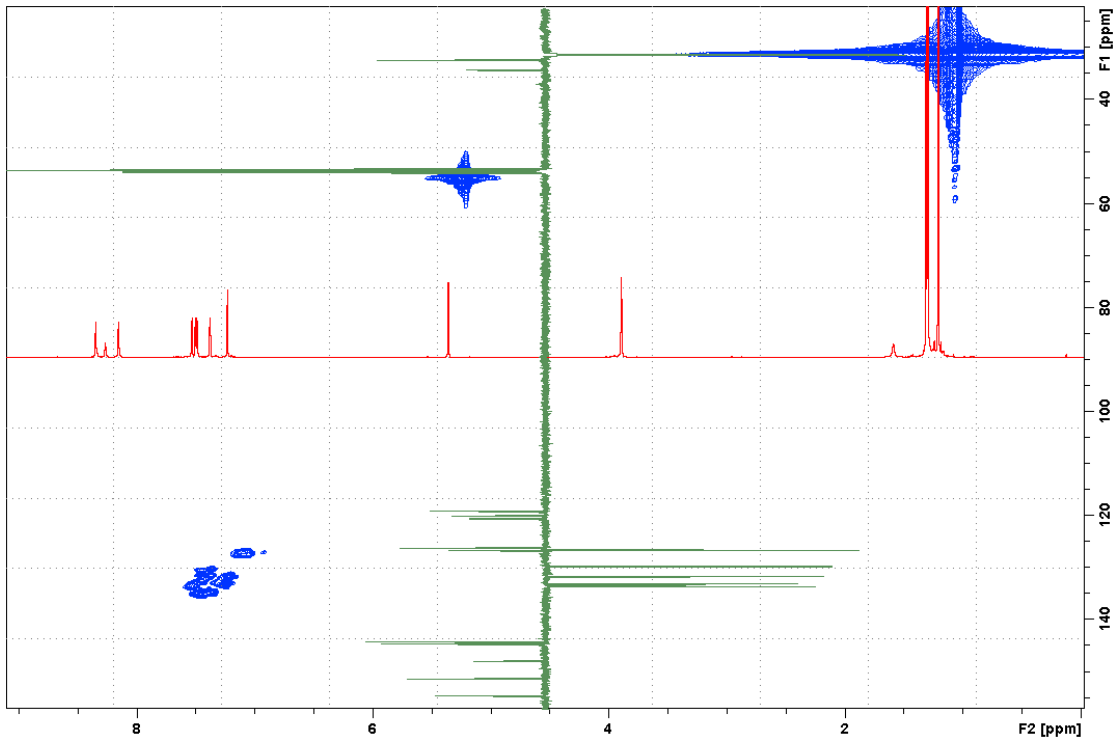


Figure 12. HMQC spectrum of compound 8

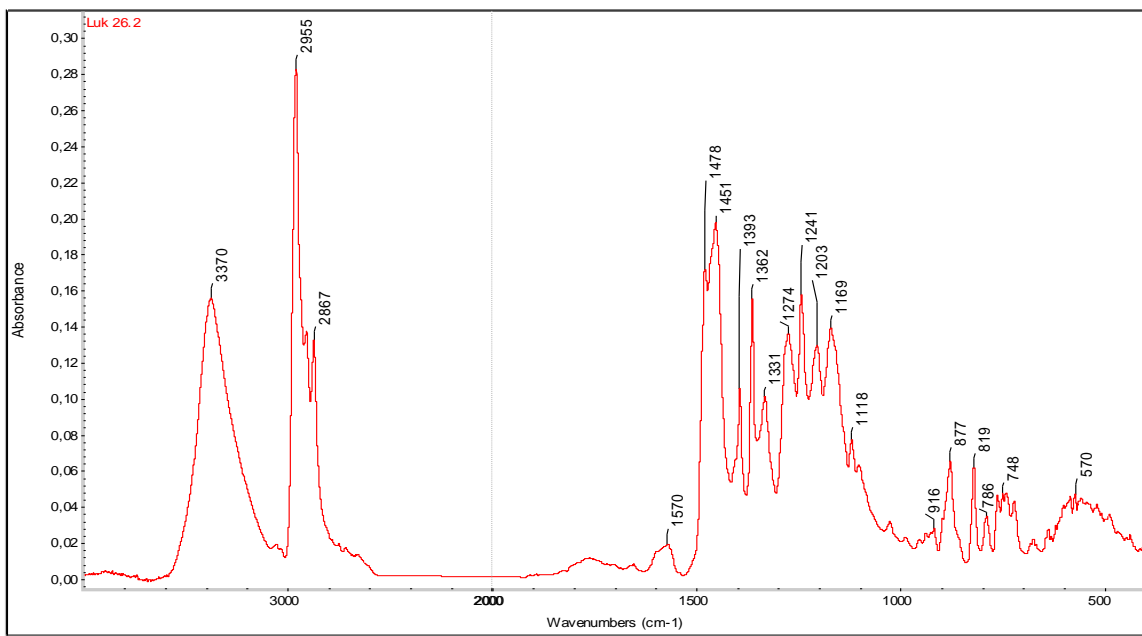


Figure 13. IR spectrum of compound **8** (ATR)

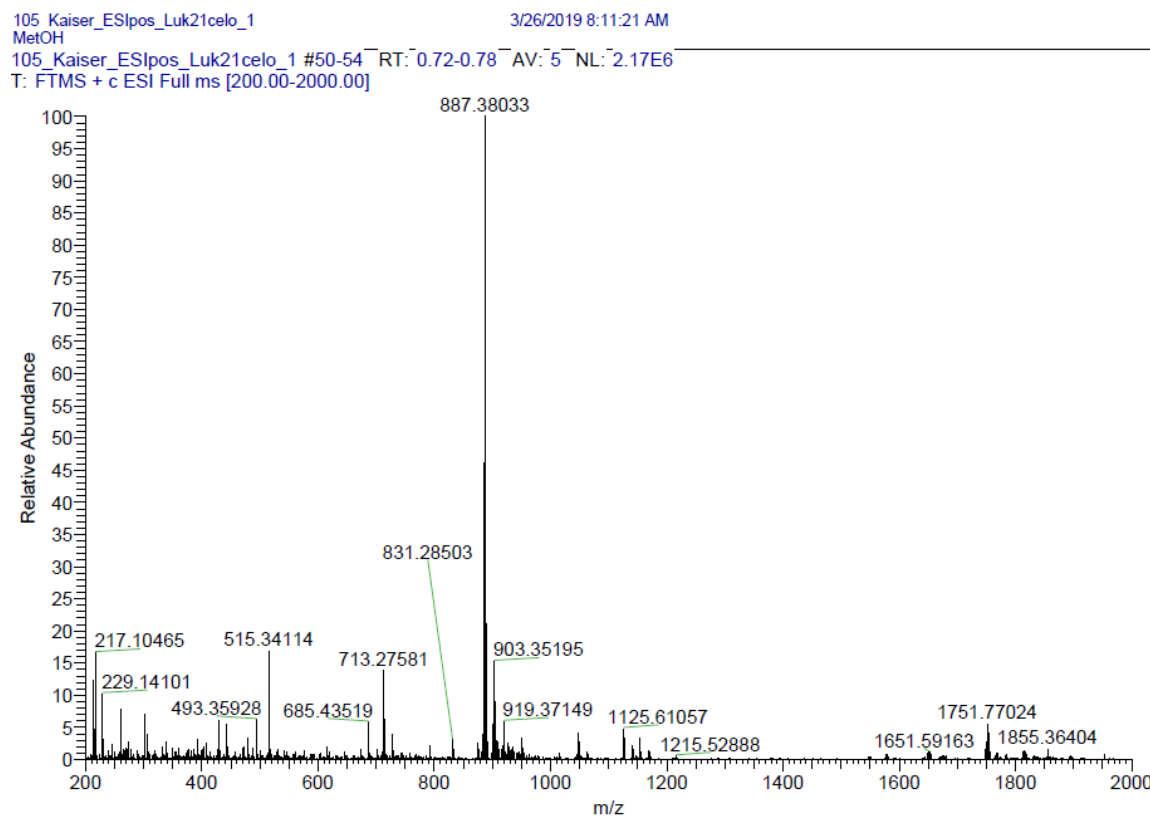
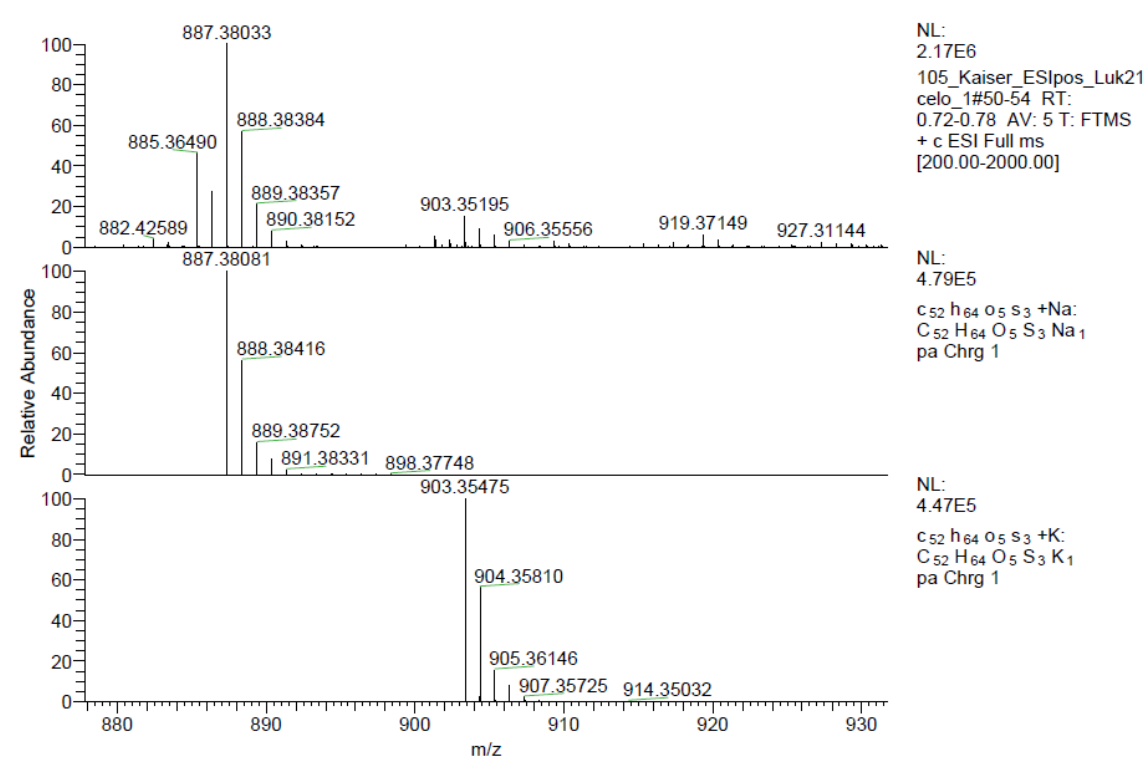
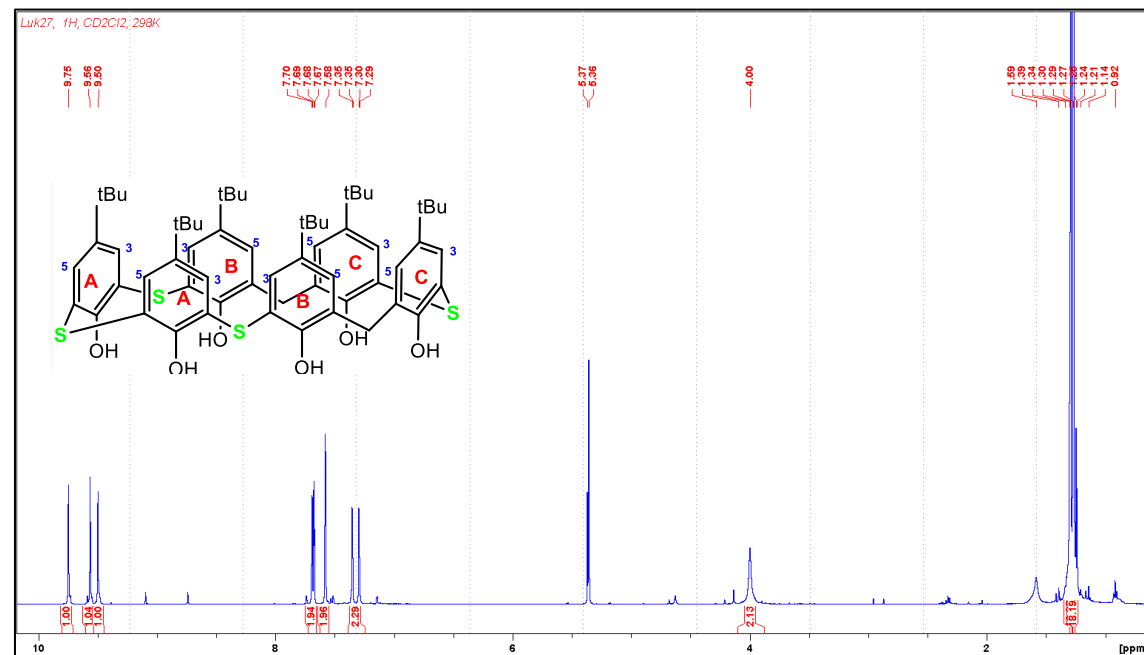


Figure 14. HRMS of compound **8** (ESI^+).

**Figure 15.** HRMS of compound 8 (ESI⁺) isotopes**Figure 16.** ¹H NMR spectrum of compound 9 (CD₂Cl₂, 600 MHz)

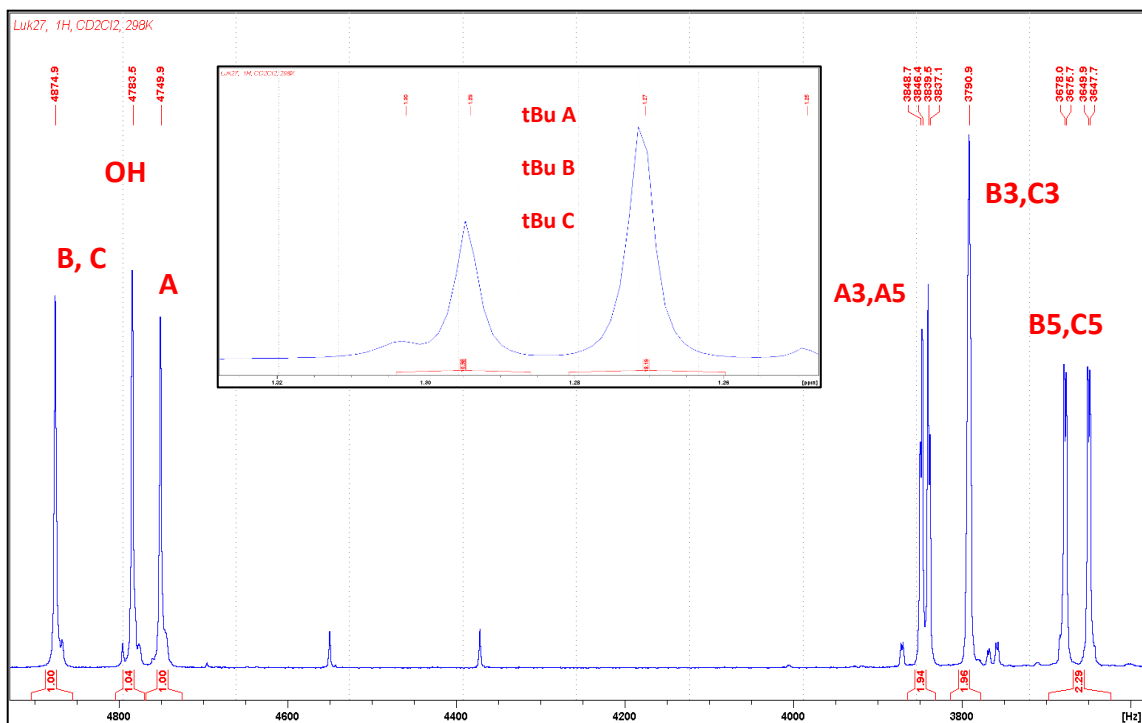


Figure 17. Assignment of ^1H NMR signals of compound **9** (CD_2Cl_2 , 600 MHz)

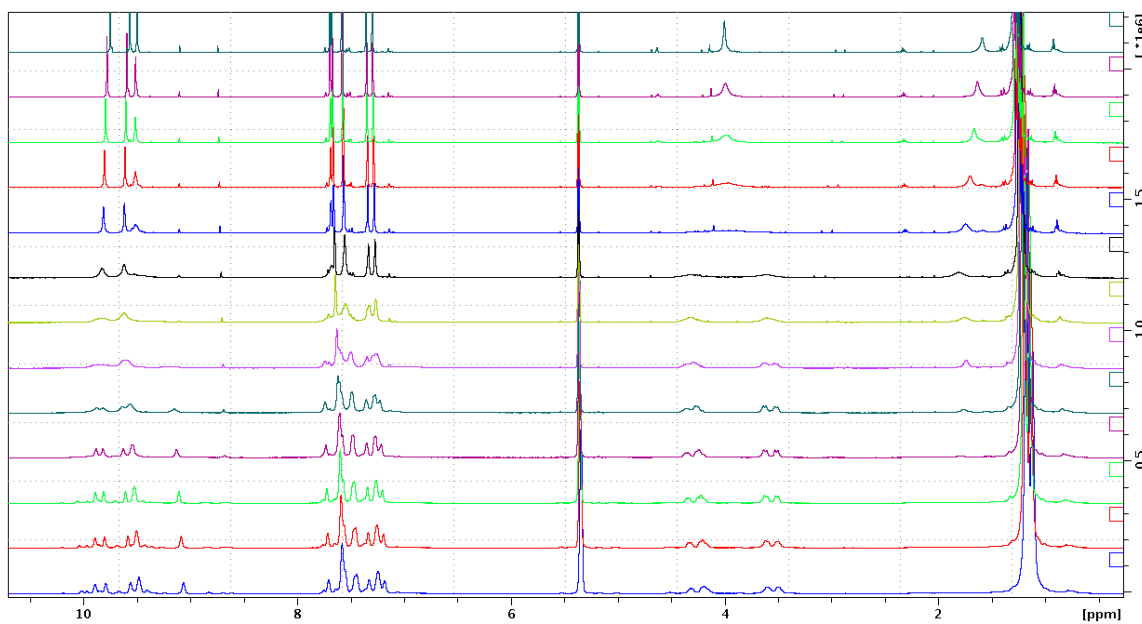


Figure 18. Variable temperature ^1H NMR experiments of compound **9** (298 – 153 K)

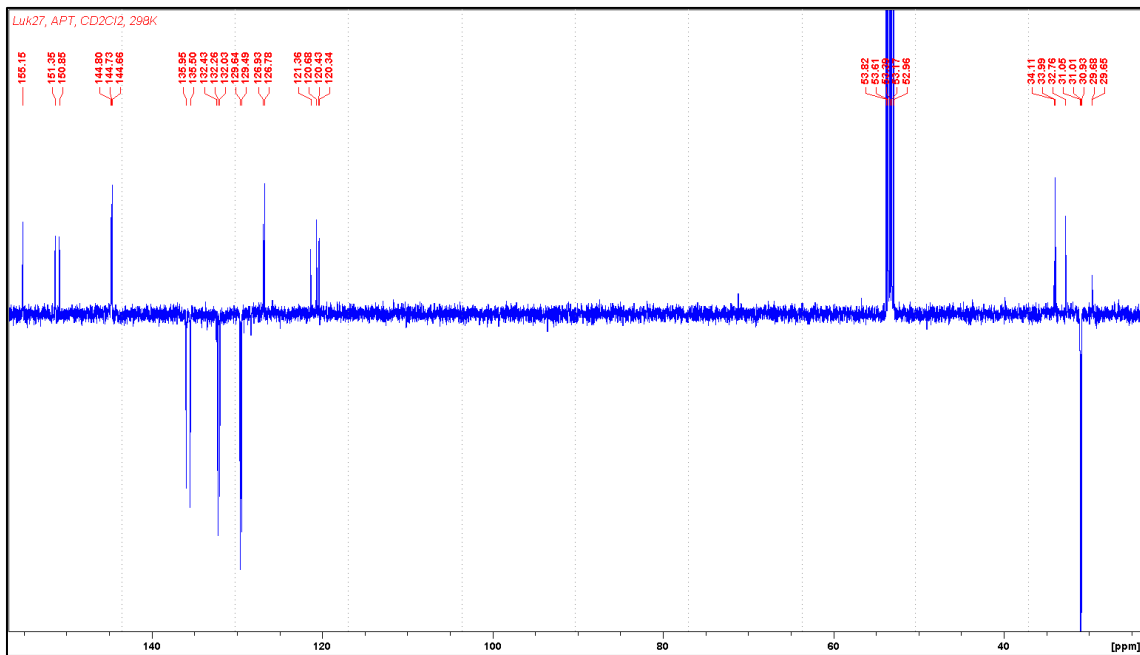


Figure 19. ^{13}C NMR spectrum of compound **9** (CD_2Cl_2 , 151 MHz)

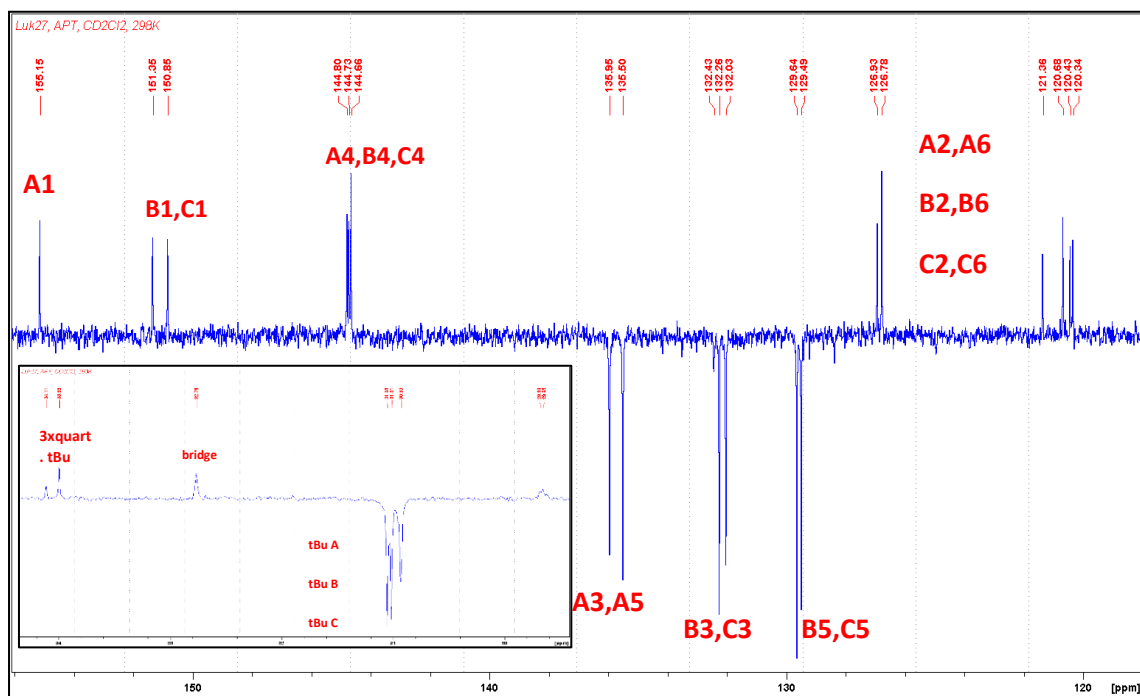


Figure 20. Assignment of ^{13}C NMR signals of compound **9** (CD_2Cl_2 , 151 MHz)

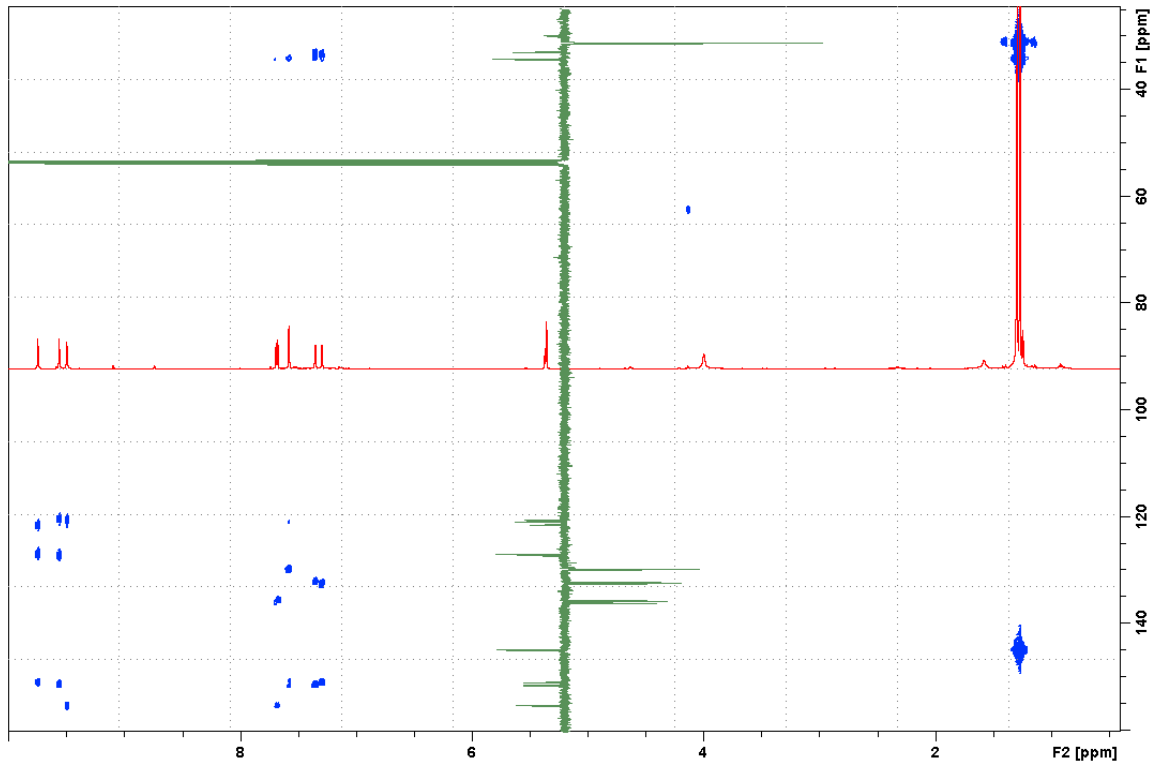


Figure 21. HMBC spectrum of compound **9**

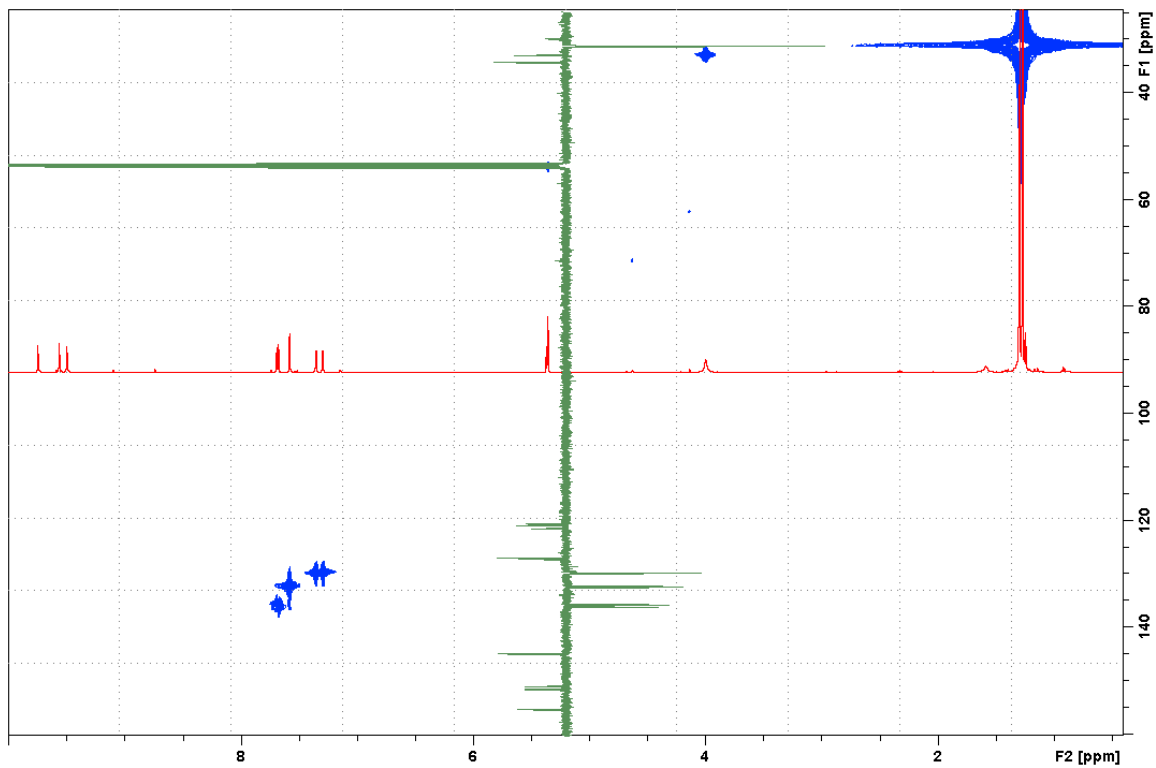


Figure 22. HMQC spectrum of compound **9**

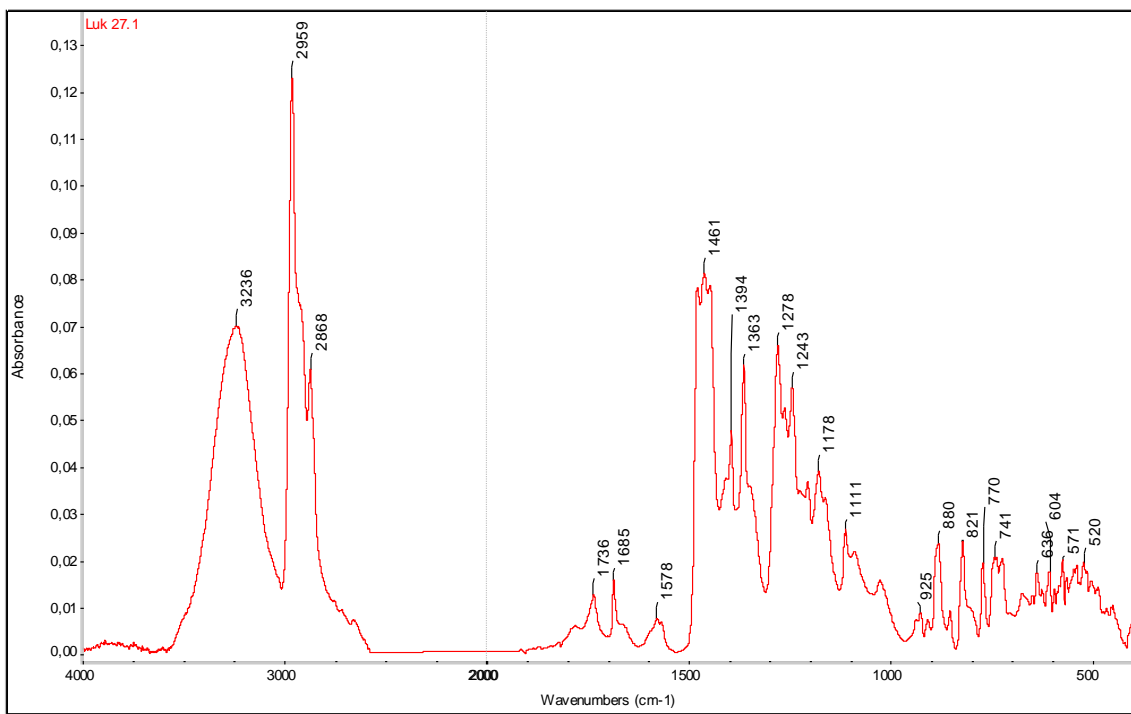


Figure 23. IR spectrum of compound **9** (ATR)

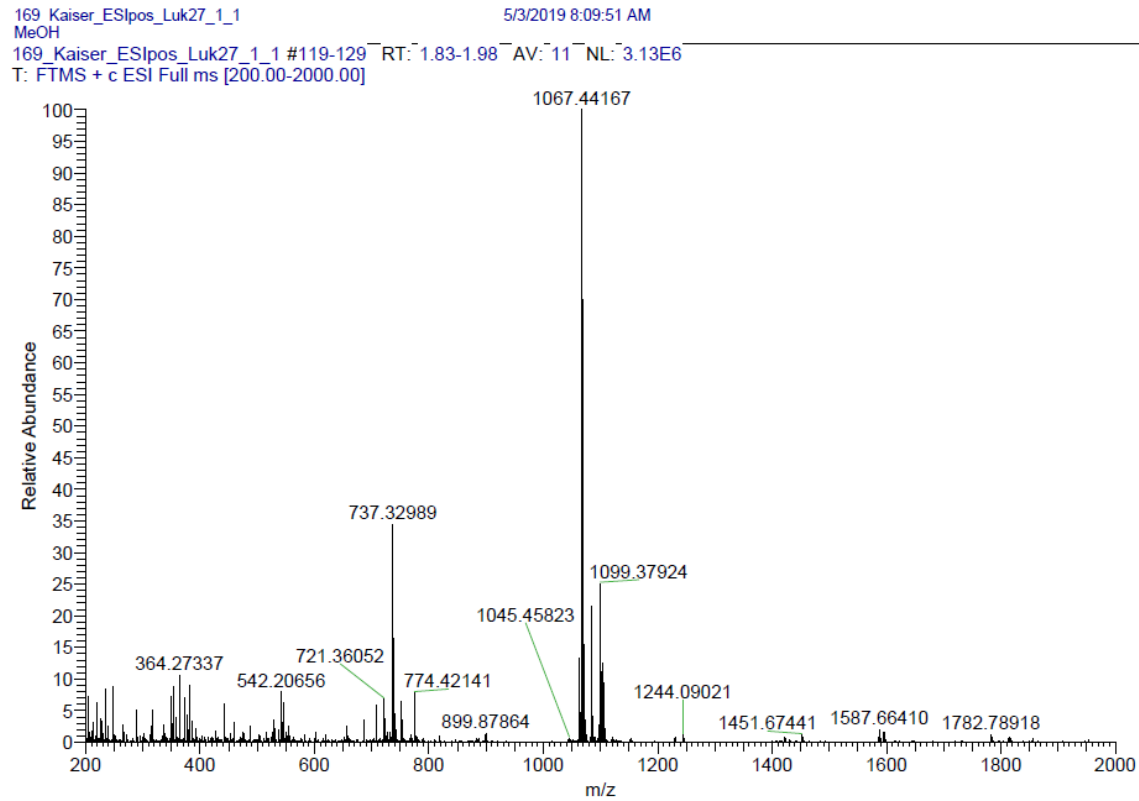
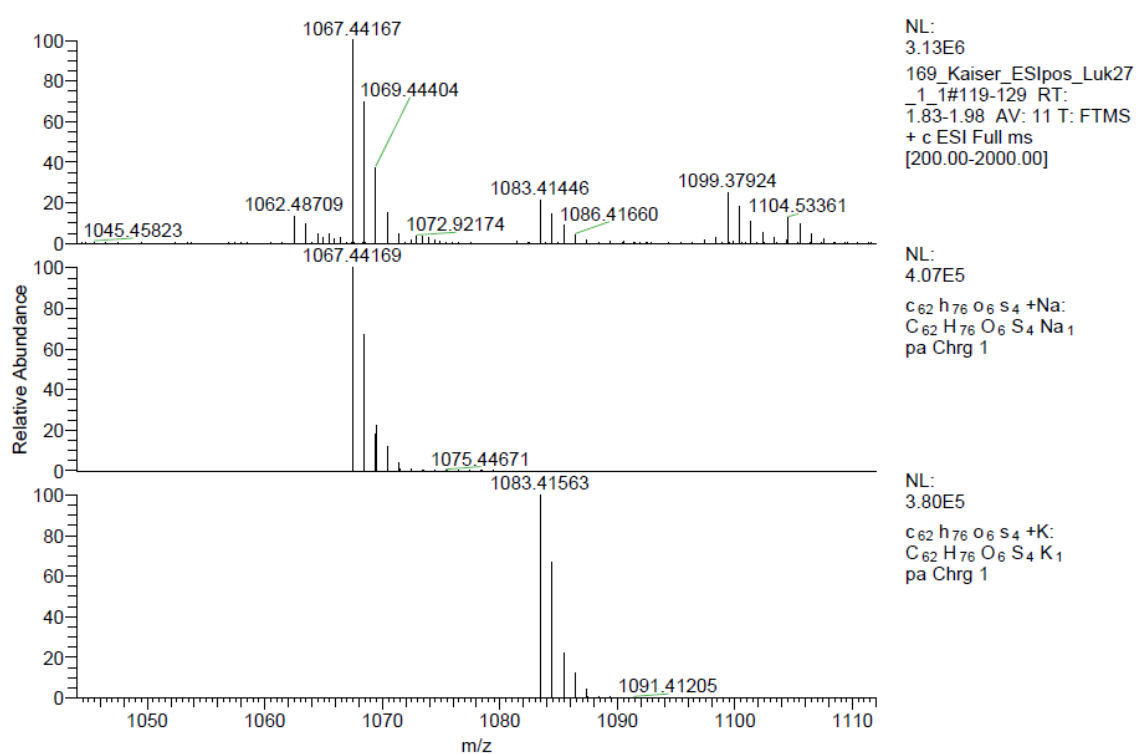
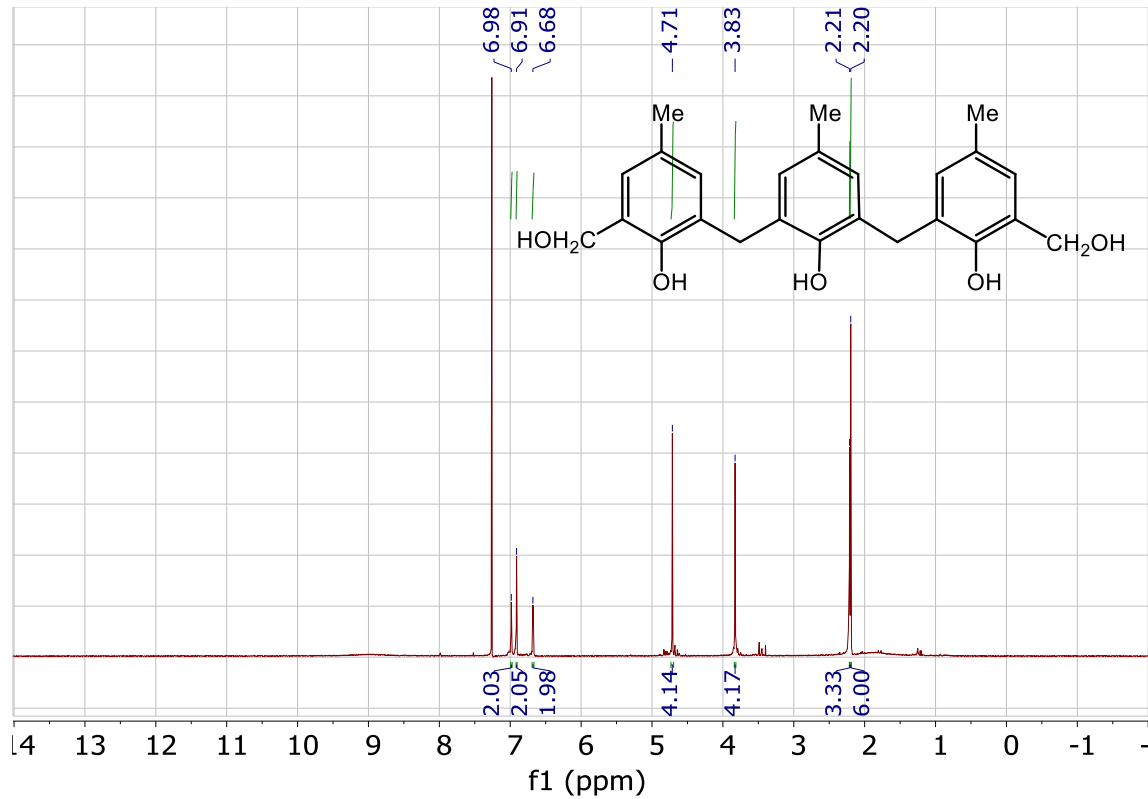


Figure 24. HRMS of compound **9** (ESI⁺).

**Figure 25.** HRMS of compound 9 (ESI^+) isotopes**Figure 26.** ^1H NMR spectrum of compound 11 (CDCl_3 , 300 MHz)

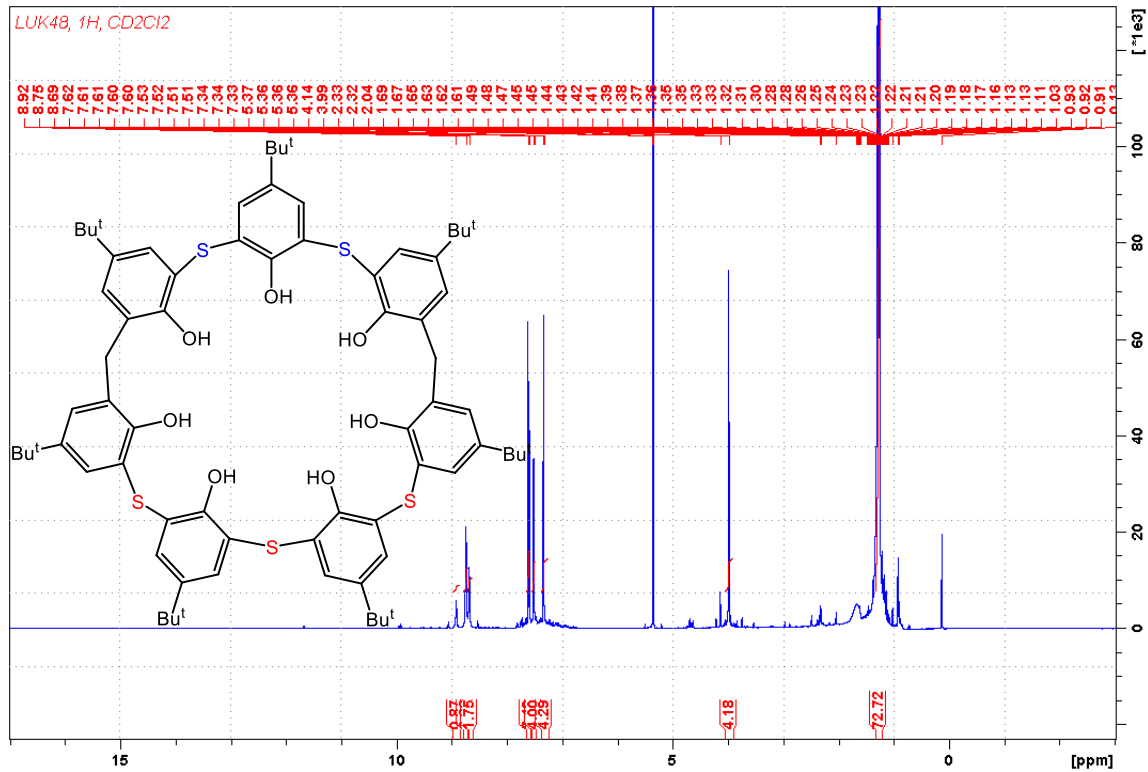


Figure 27. ^1H NMR spectrum of compound **12** (CD_2Cl_2 , 600 MHz)

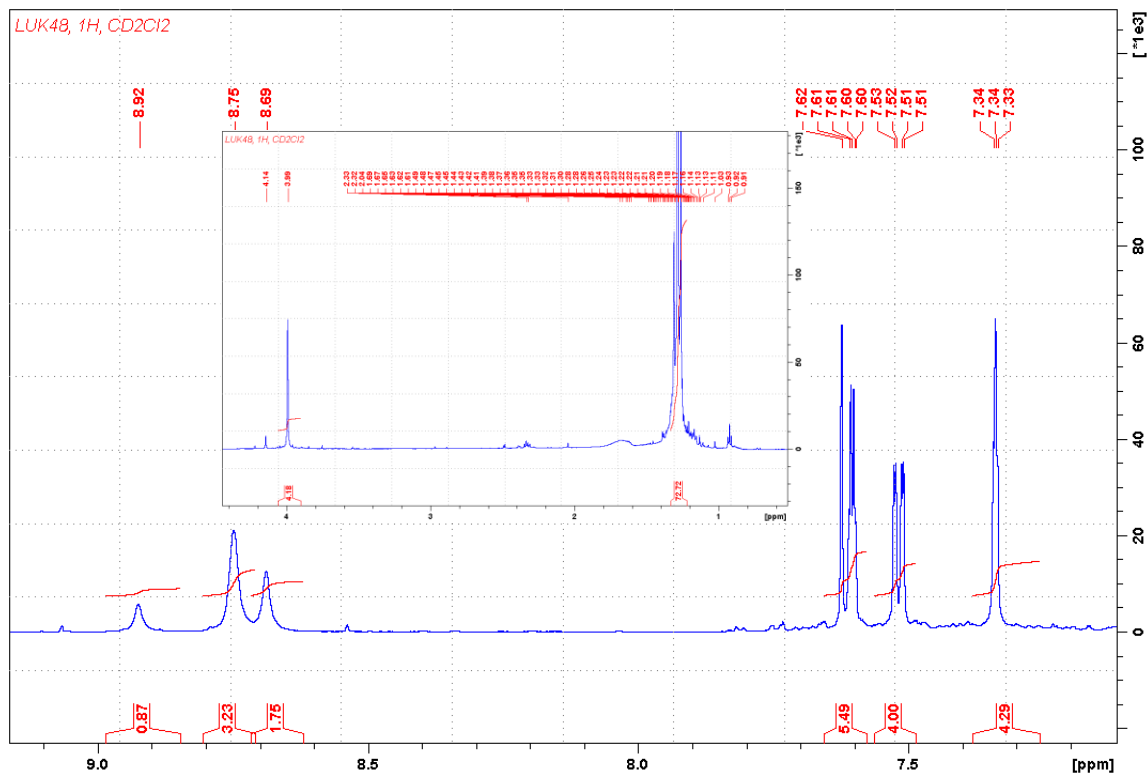


Figure 28. ^1H NMR spectrum of compound **12** (CD_2Cl_2 , 600 MHz) with detail of aromatic and aliphatic section

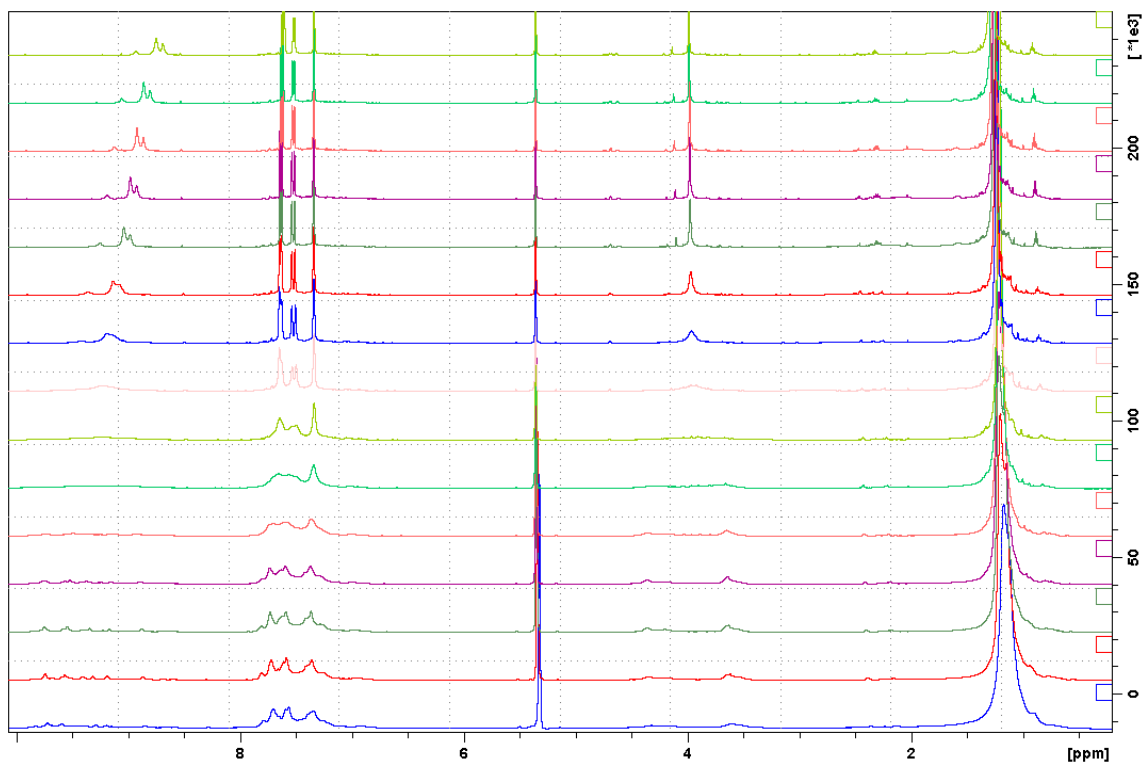


Figure 29. Variable temperature ¹H NMR experiments of compound **12** (298 – 153 K)

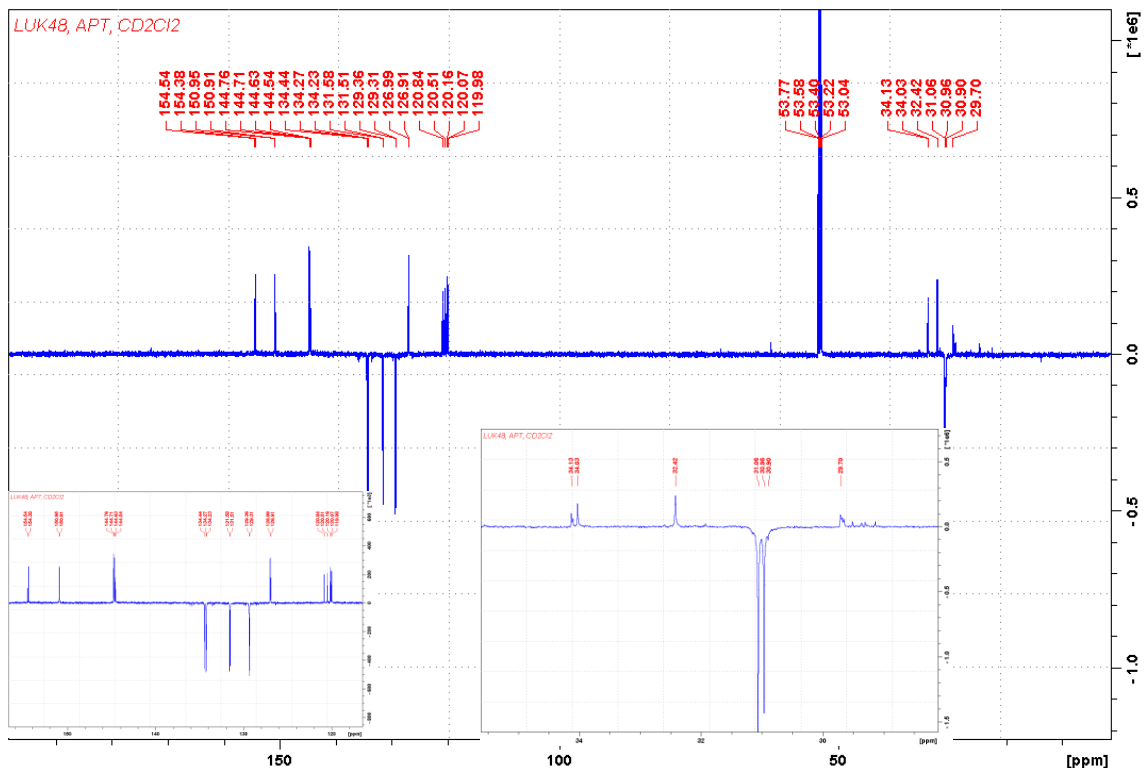


Figure 30. ¹³C NMR spectrum of compound **12** (CD_2Cl_2 , 151 MHz)

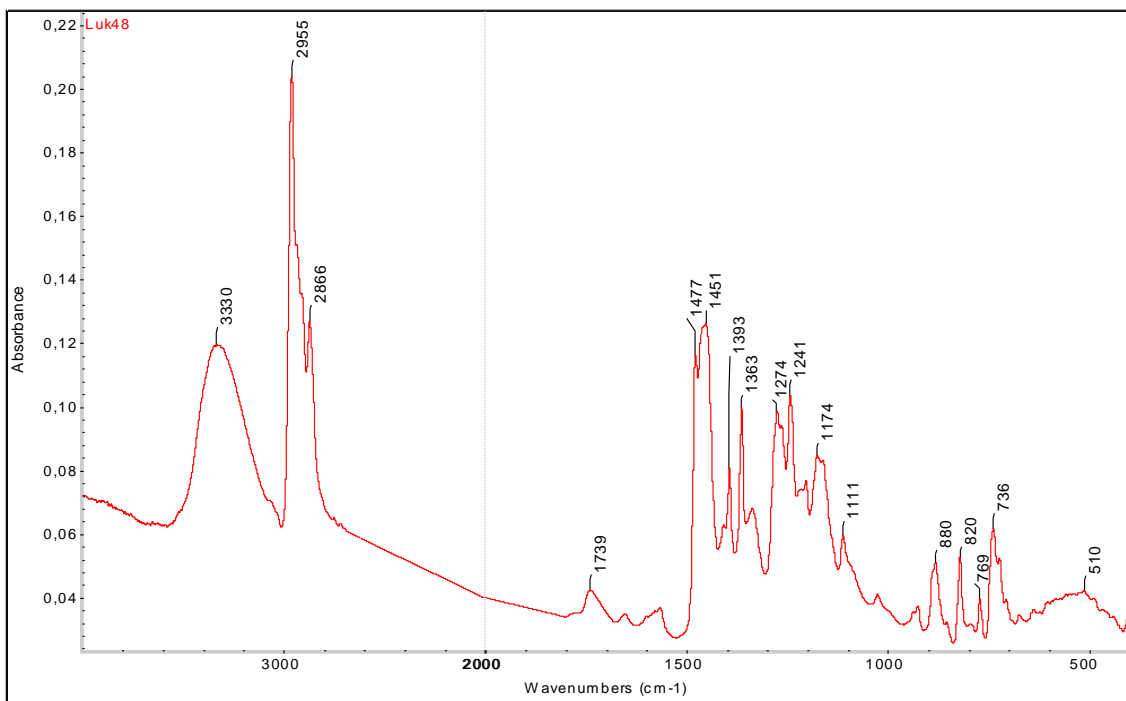


Figure 31. IR spectrum of compound **12** (ATR)

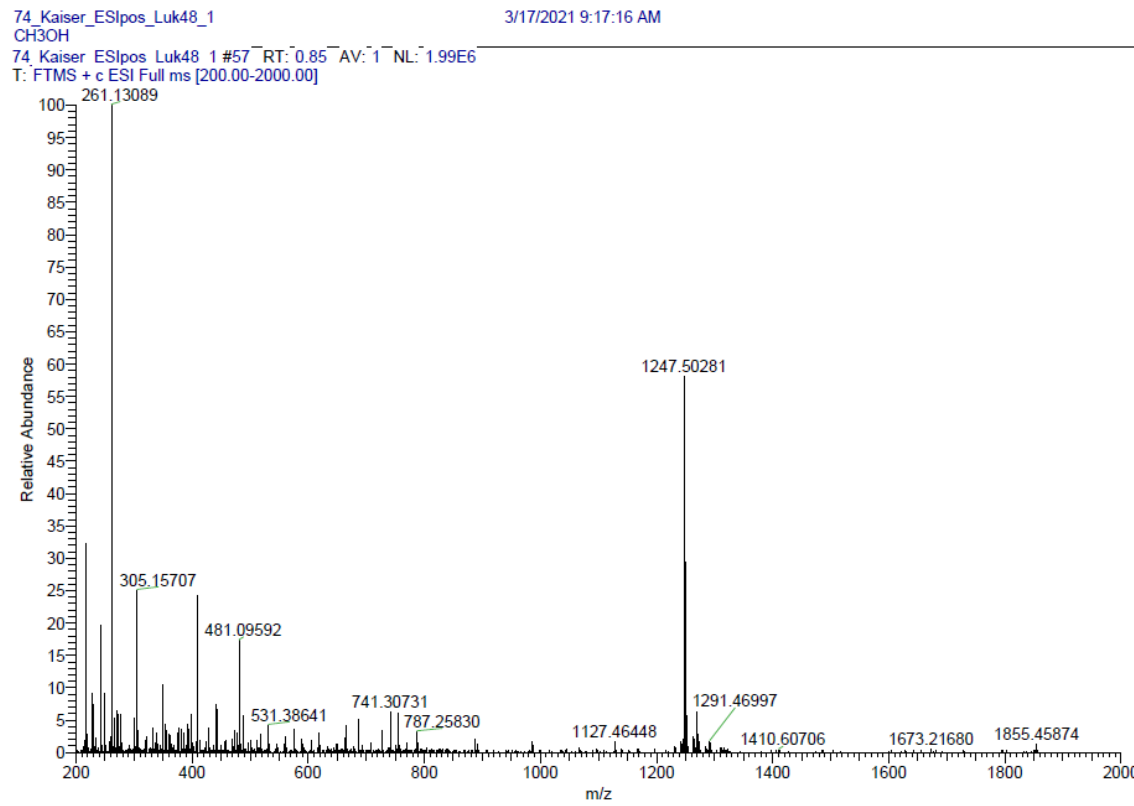
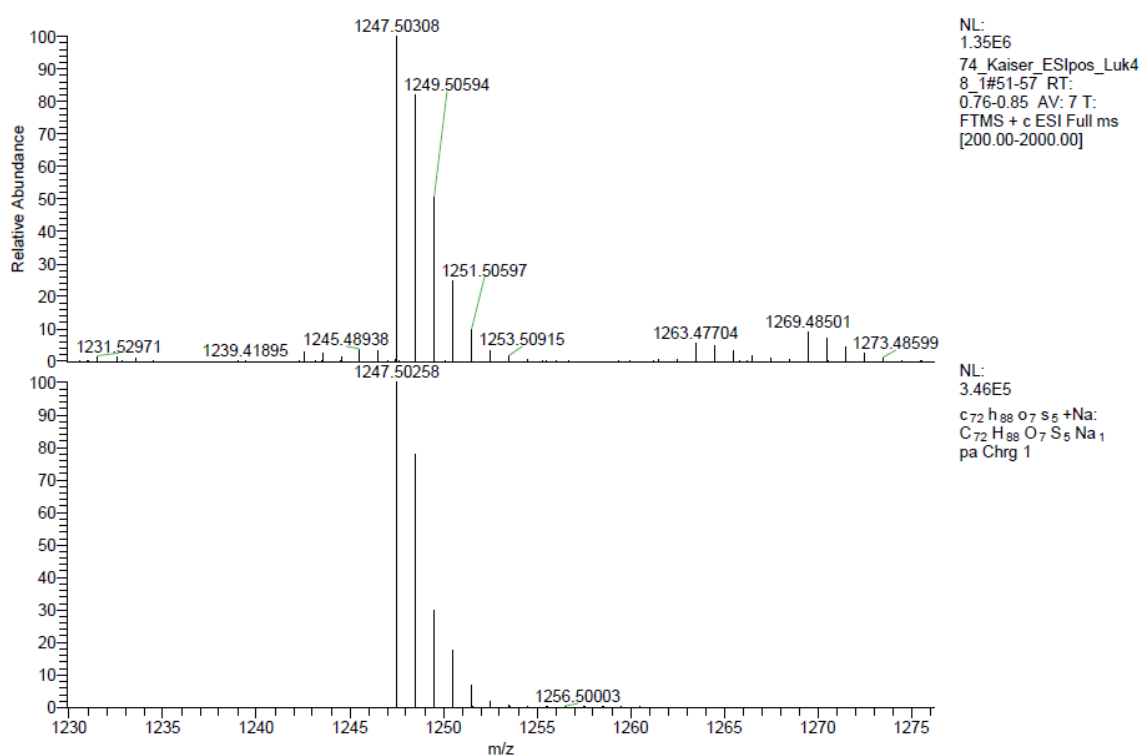
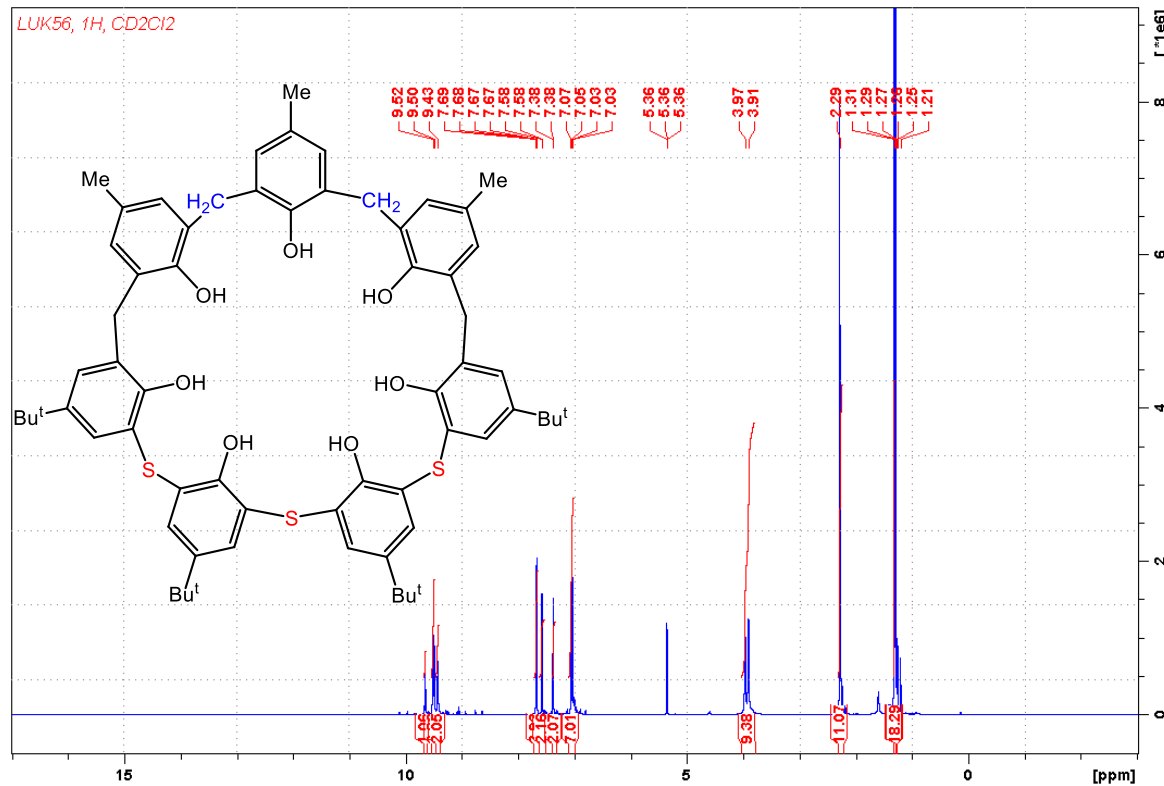


Figure 32. HRMS of compound **12** (ESI^+).

**Figure 33.** HRMS of compound **12** (ESI^+) isotopes**Figure 34.** 1H NMR spectrum of compound **13** (CD₂Cl₂, 600 MHz)

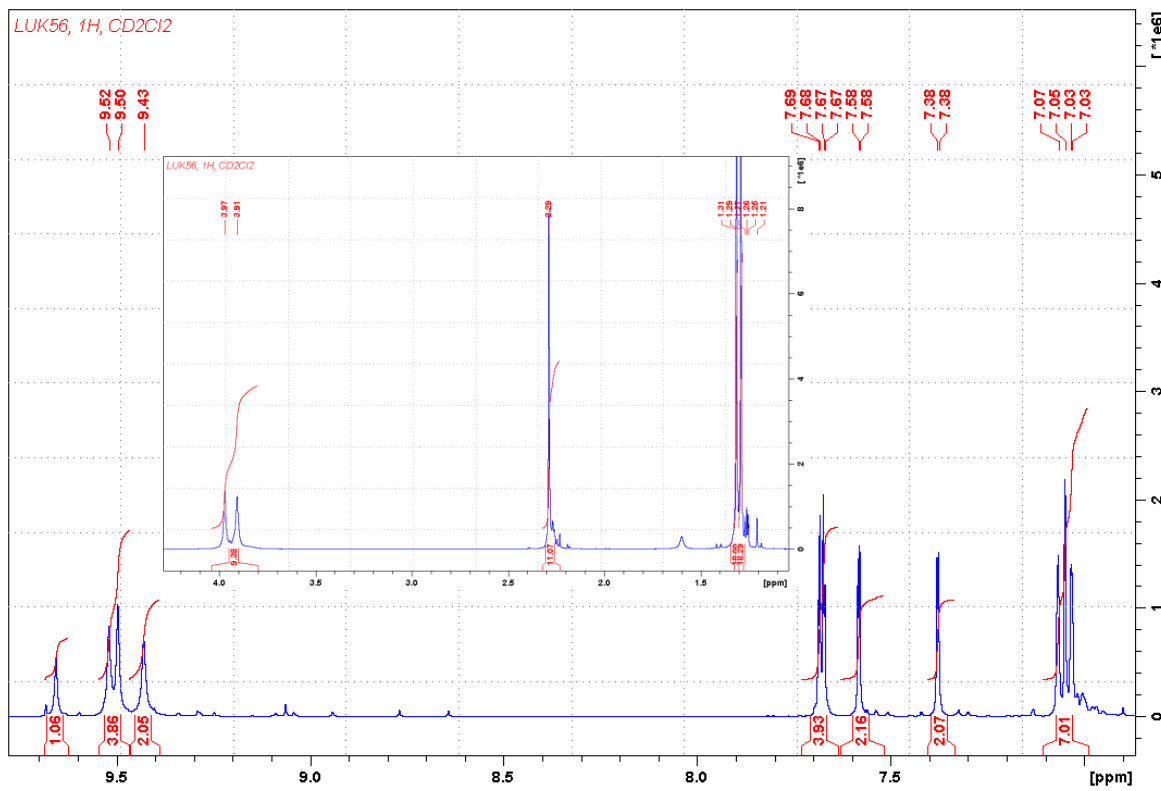


Figure 35. ^1H NMR spectrum of compound **13** (CD_2Cl_2 , 600 MHz) with detail of aromatic and aliphatic section

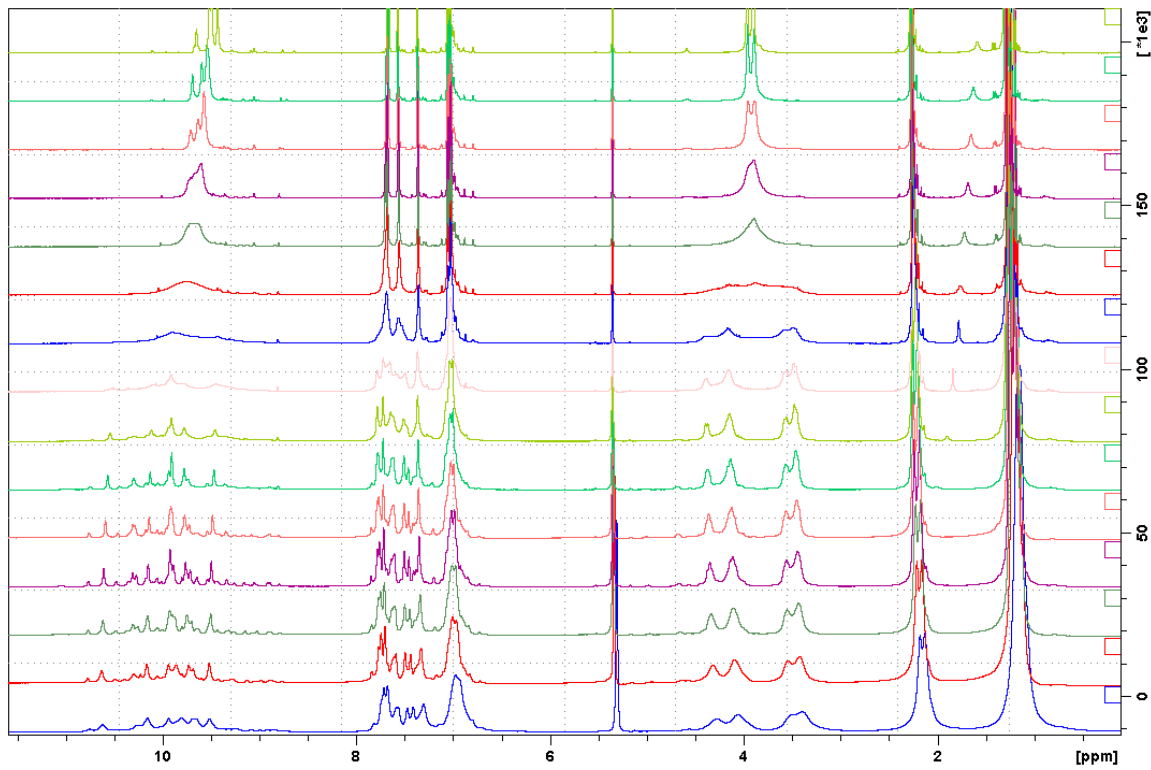


Figure 36. Variable temperature ^1H NMR experiments of compound **13** (298 – 153 K)

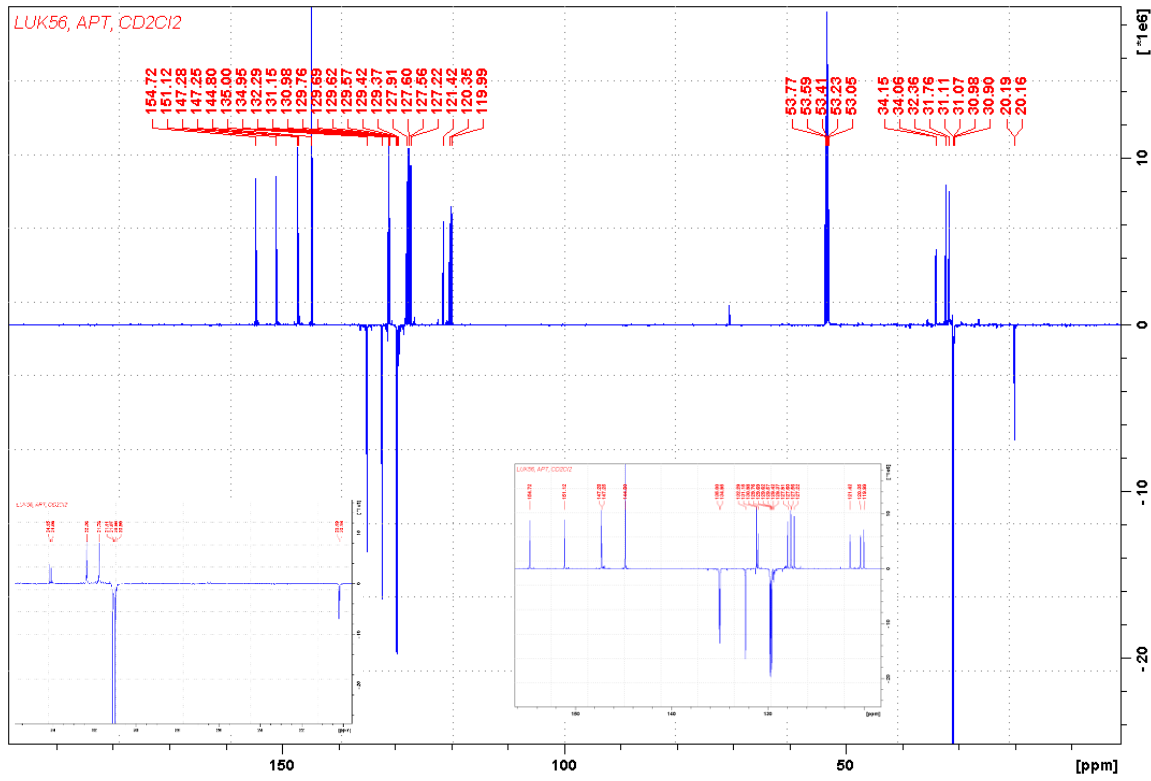


Figure 37. ^{13}C NMR spectrum of compound **13** (CD_2Cl_2 , 151 MHz)

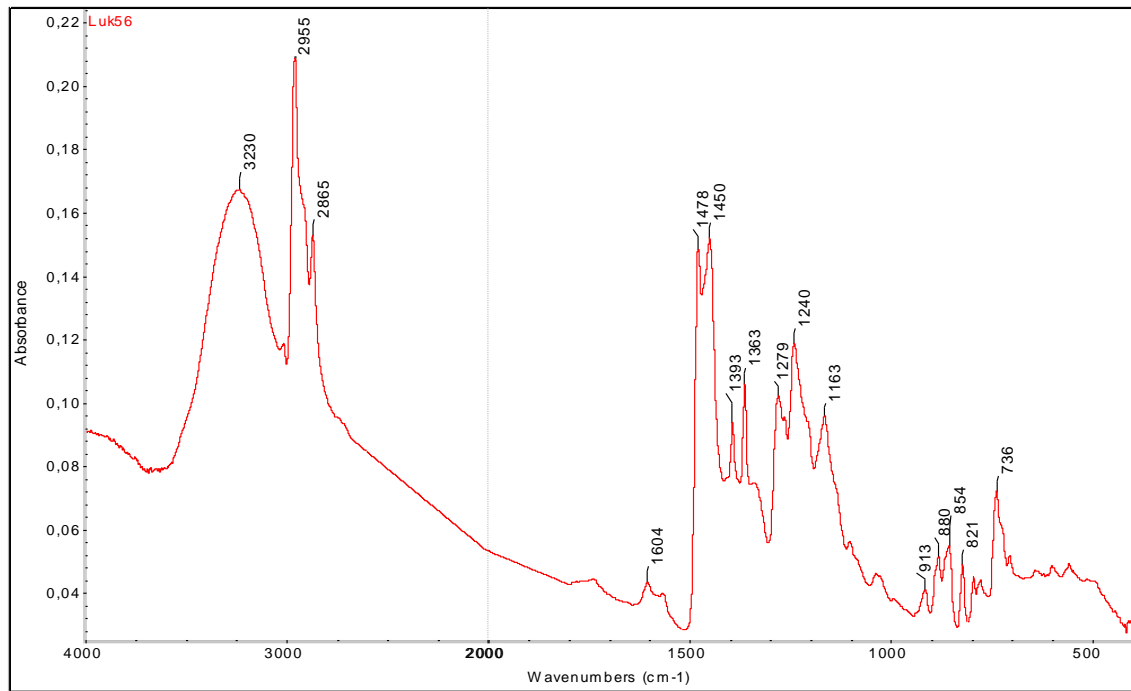


Figure 38. IR spectrum of compound **13** (ATR)

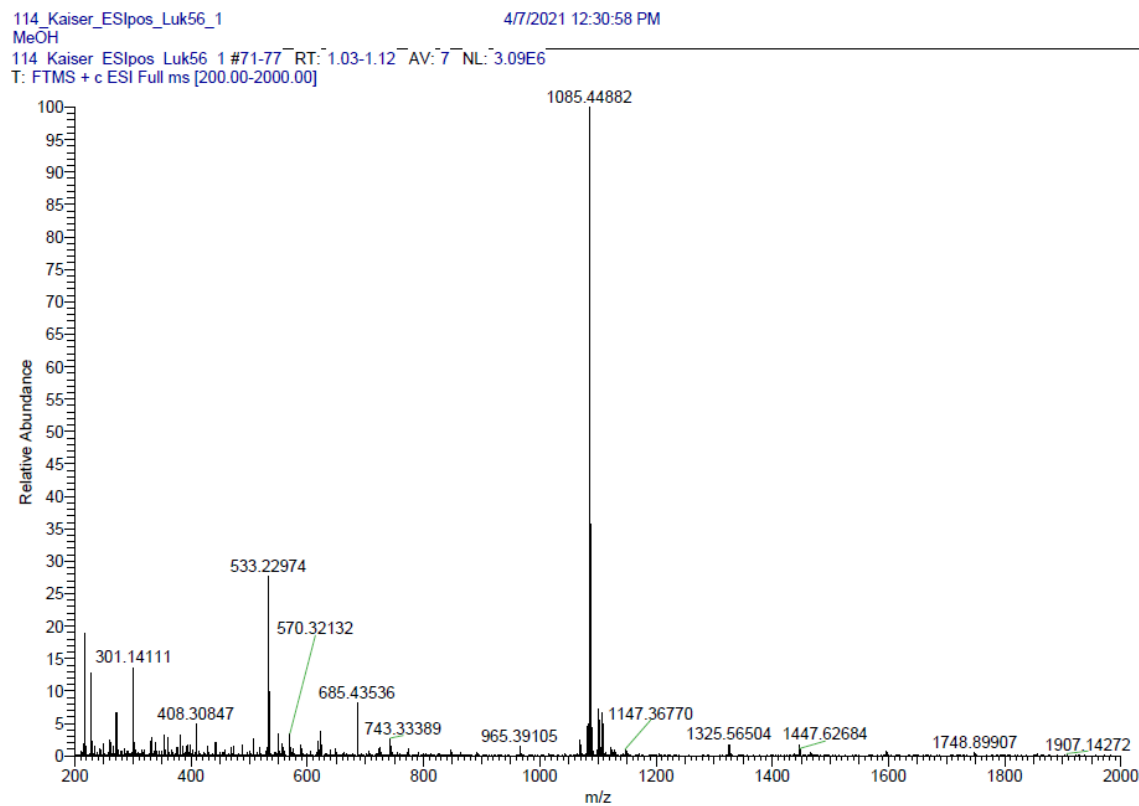


Figure 39. HRMS of compound 13 (ESI⁺)

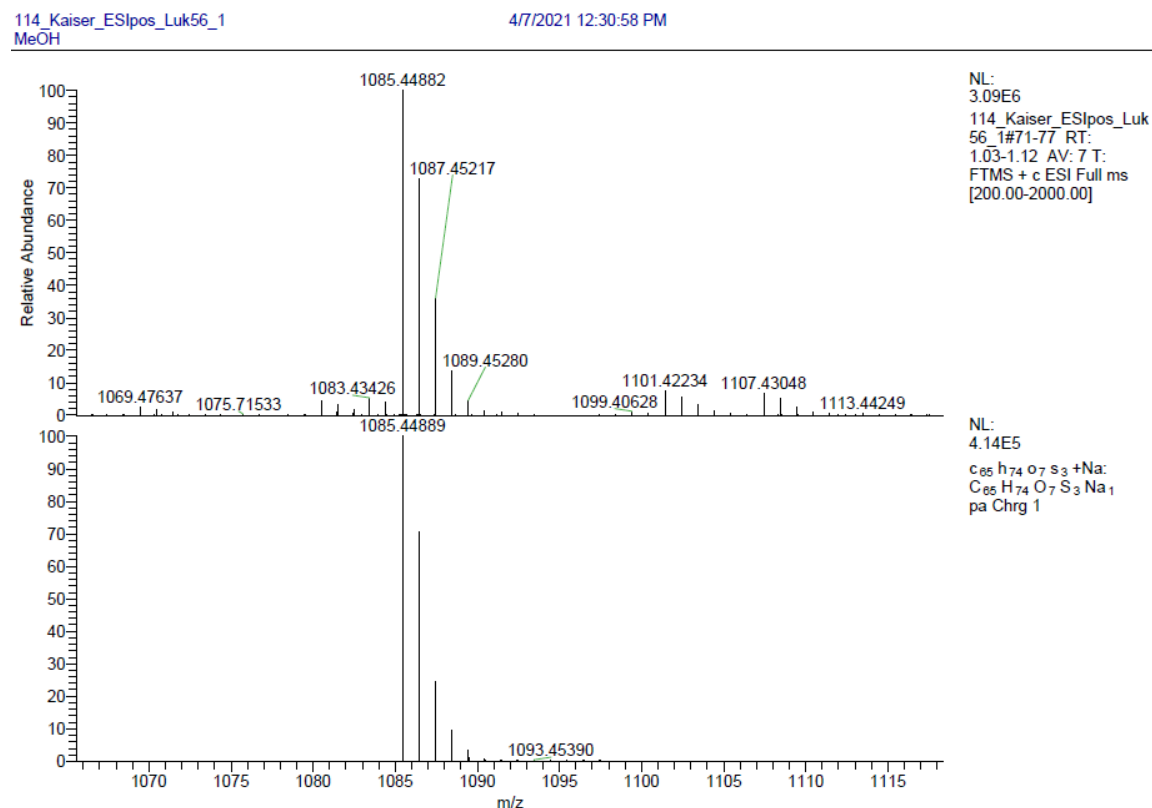


Figure 40. HRMS of compound 13 (ESI⁺) isotopes

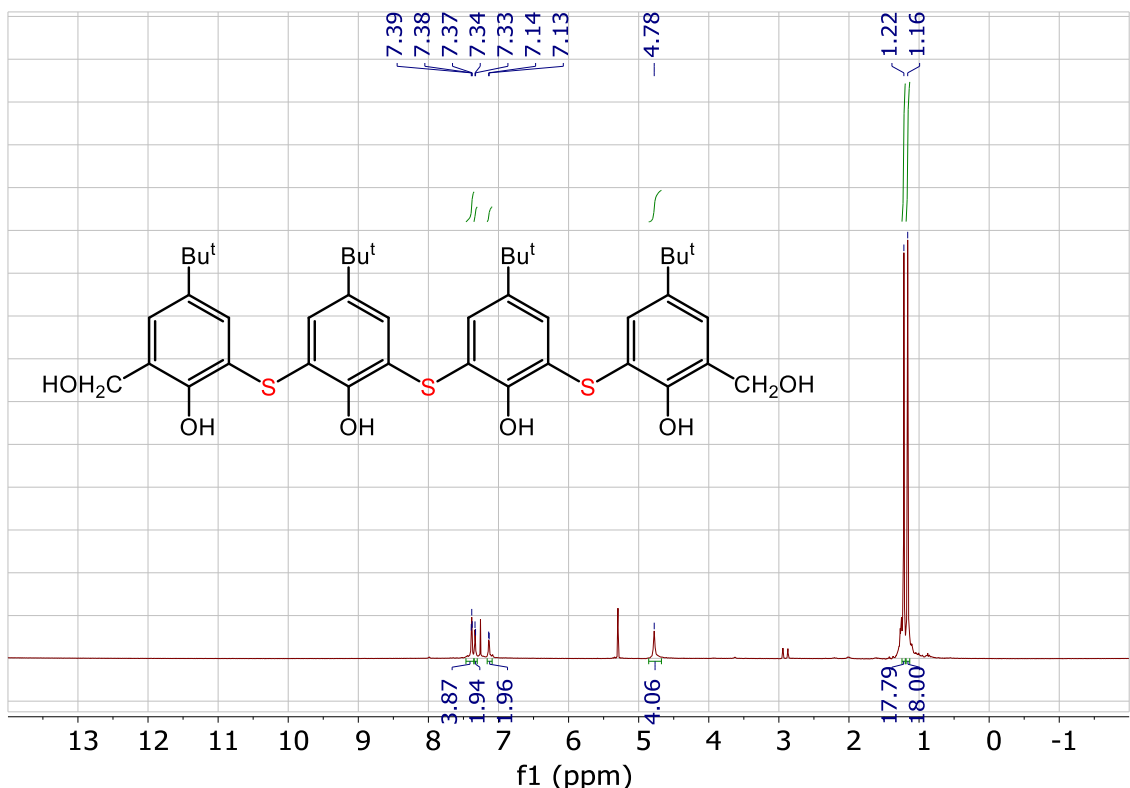


Figure 41. ^1H NMR spectrum of compound **14** (CDCl_3 , 400 MHz)

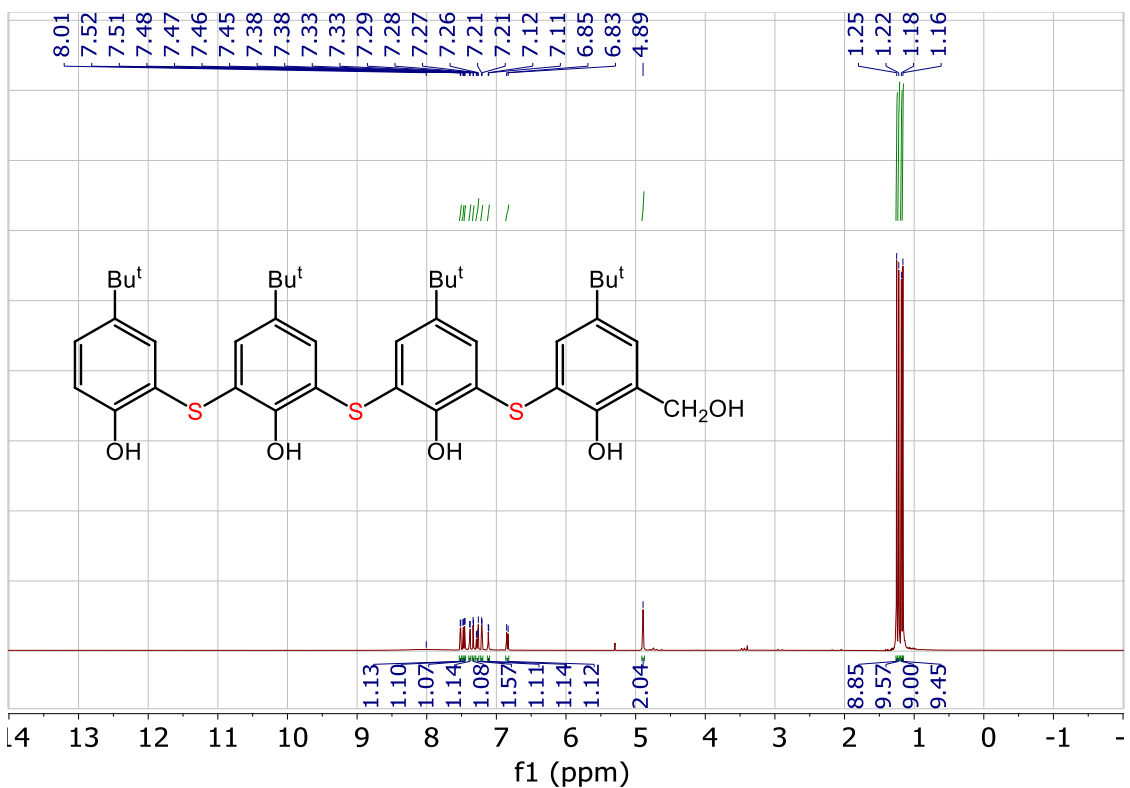


Figure 42. ^1H NMR spectrum of compound **15** (CDCl_3 , 400 MHz)

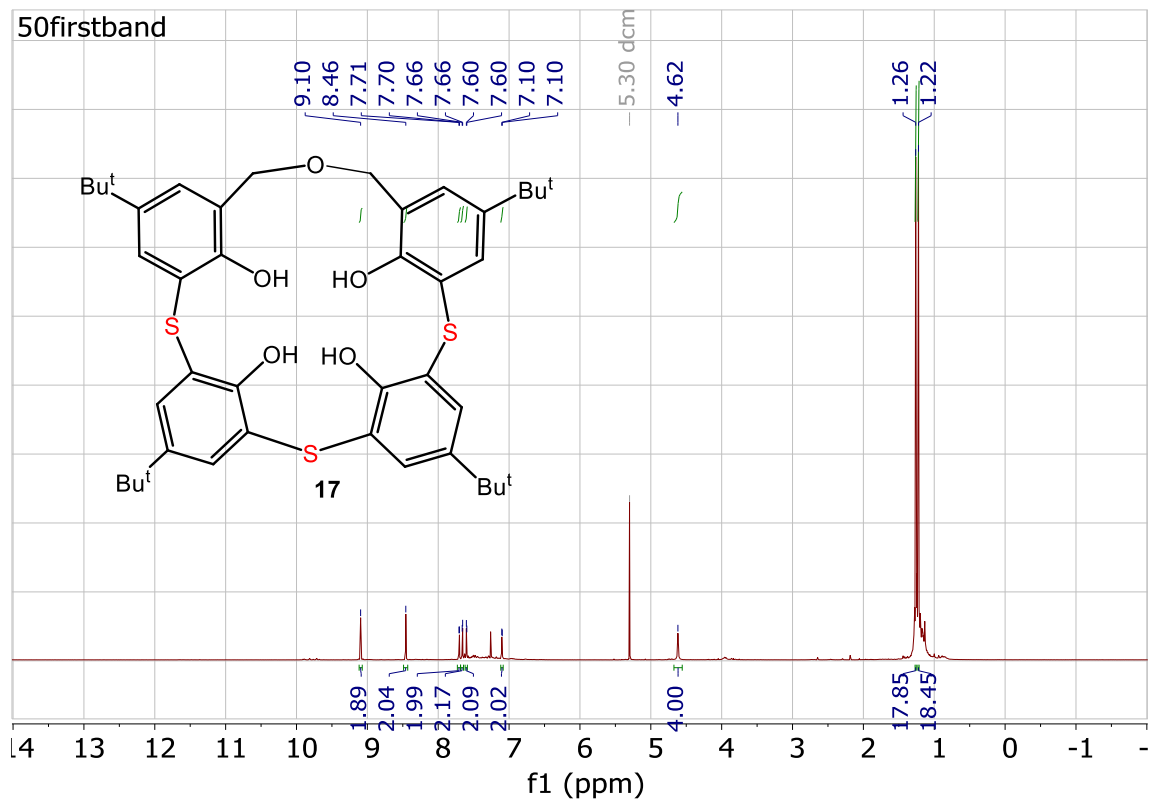


Figure 43. ^1H NMR spectrum of compound **17** (CDCl_3 , 400 MHz)

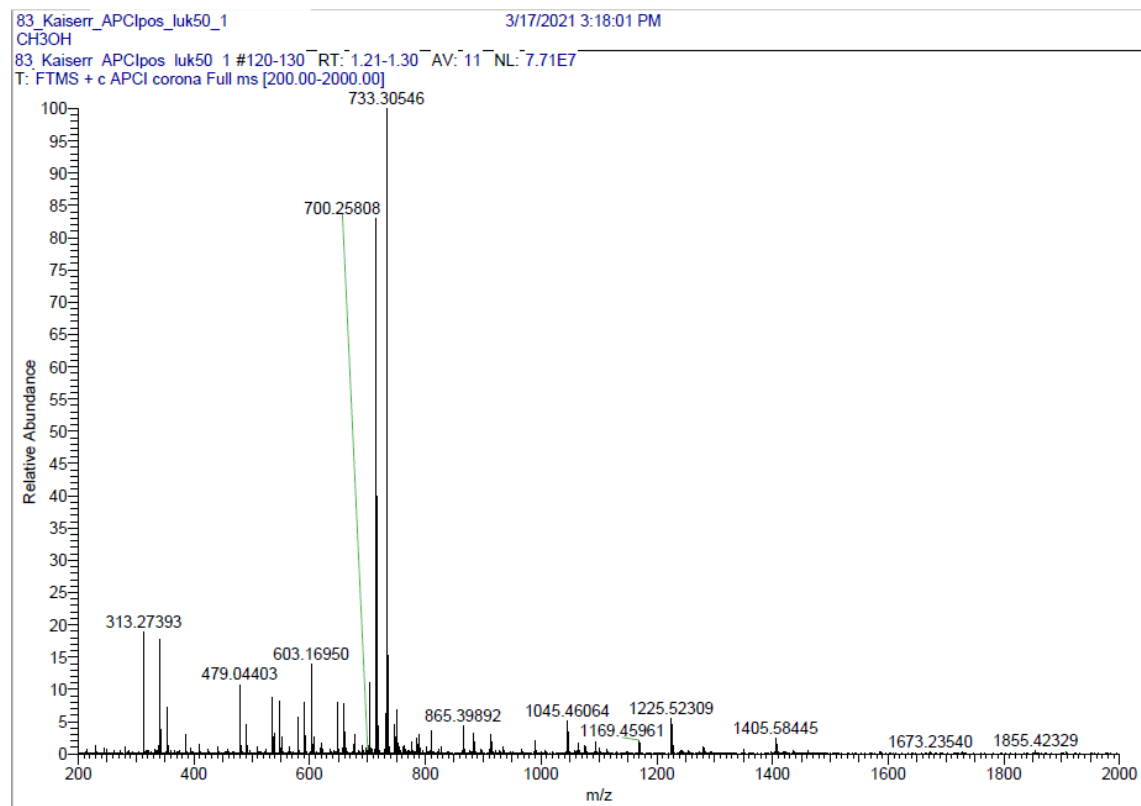
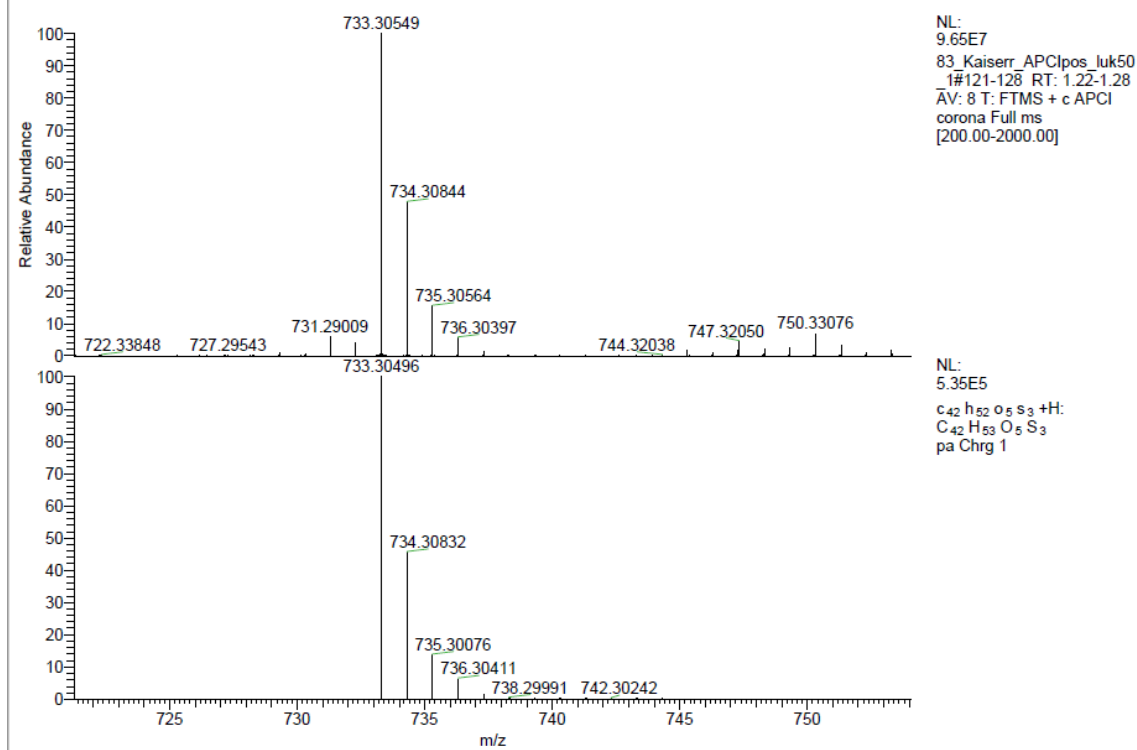
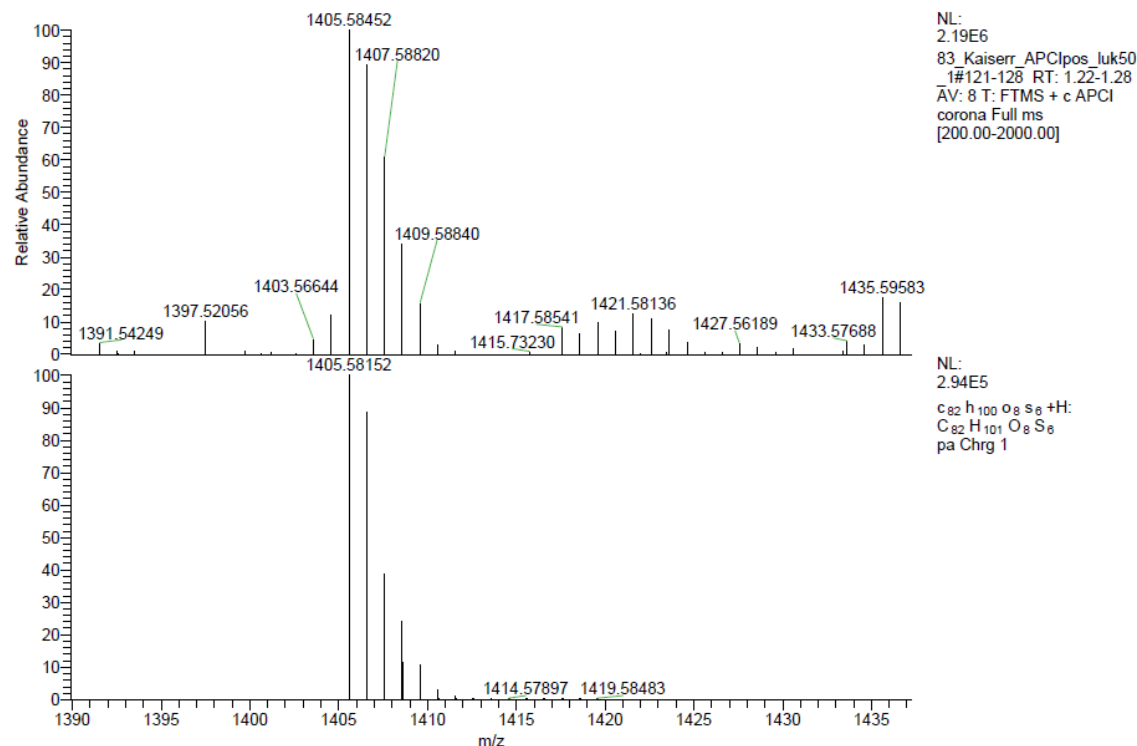


Figure 44. HRMS of compound **17** (ESI^+)

**Figure 45.** HRMS of compound 17 (ESI^+) isotopes**Figure 46.** HRMS of compound 17 (ESI^+) dimer isotopes

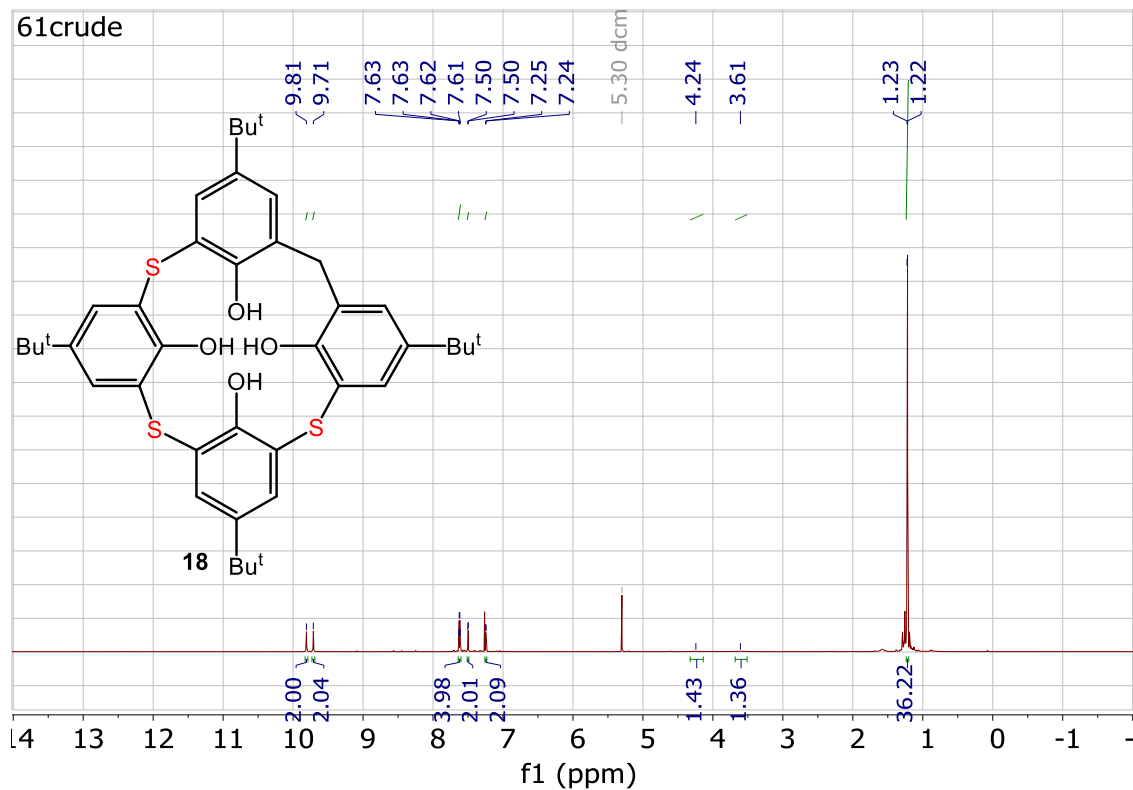


Figure 47. ^1H NMR spectrum of compound **18** (CDCl_3 , 400 MHz)

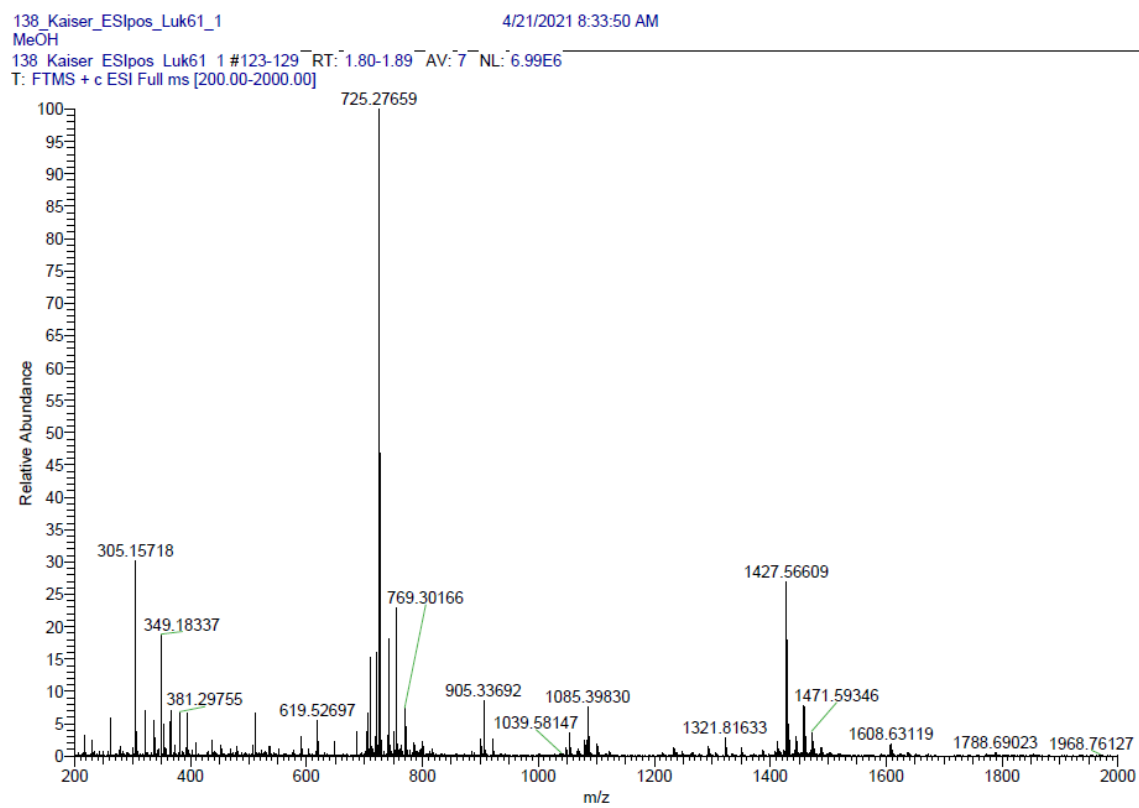


Figure 48. HRMS of compound **18** (ESI^+)

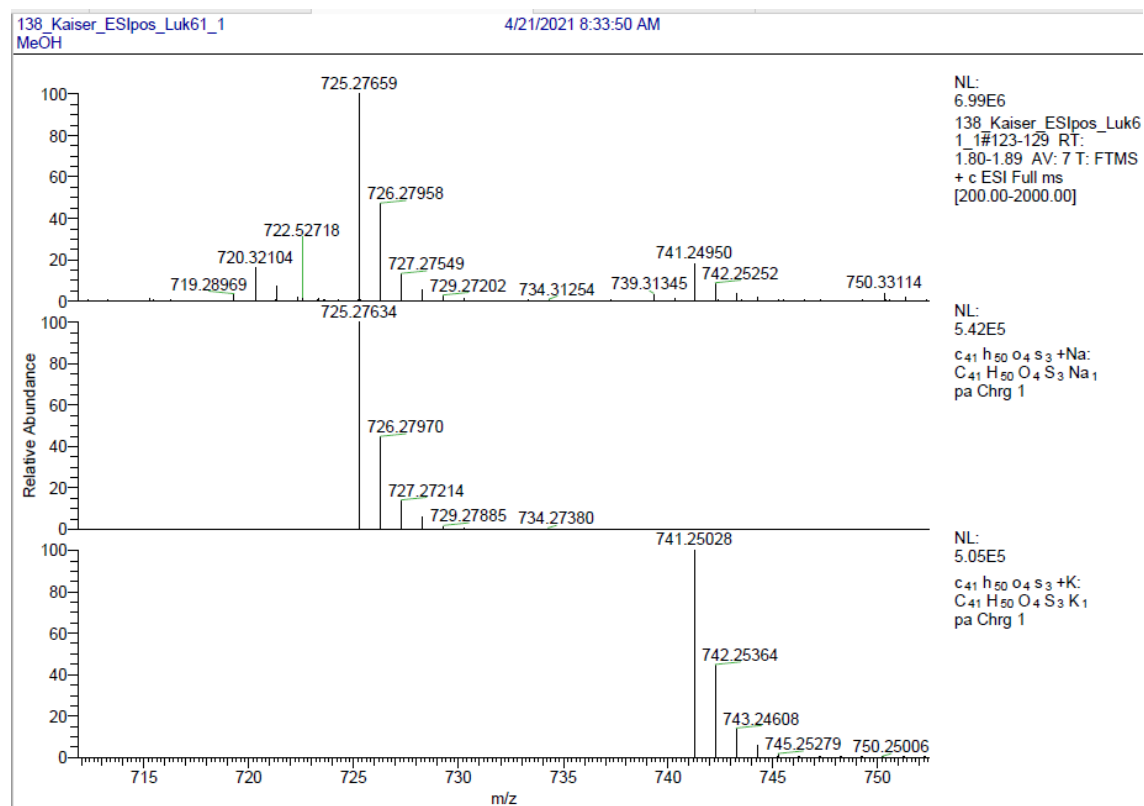


Figure 49. HRMS of compound 18 (ESI⁺) isotopes monomer

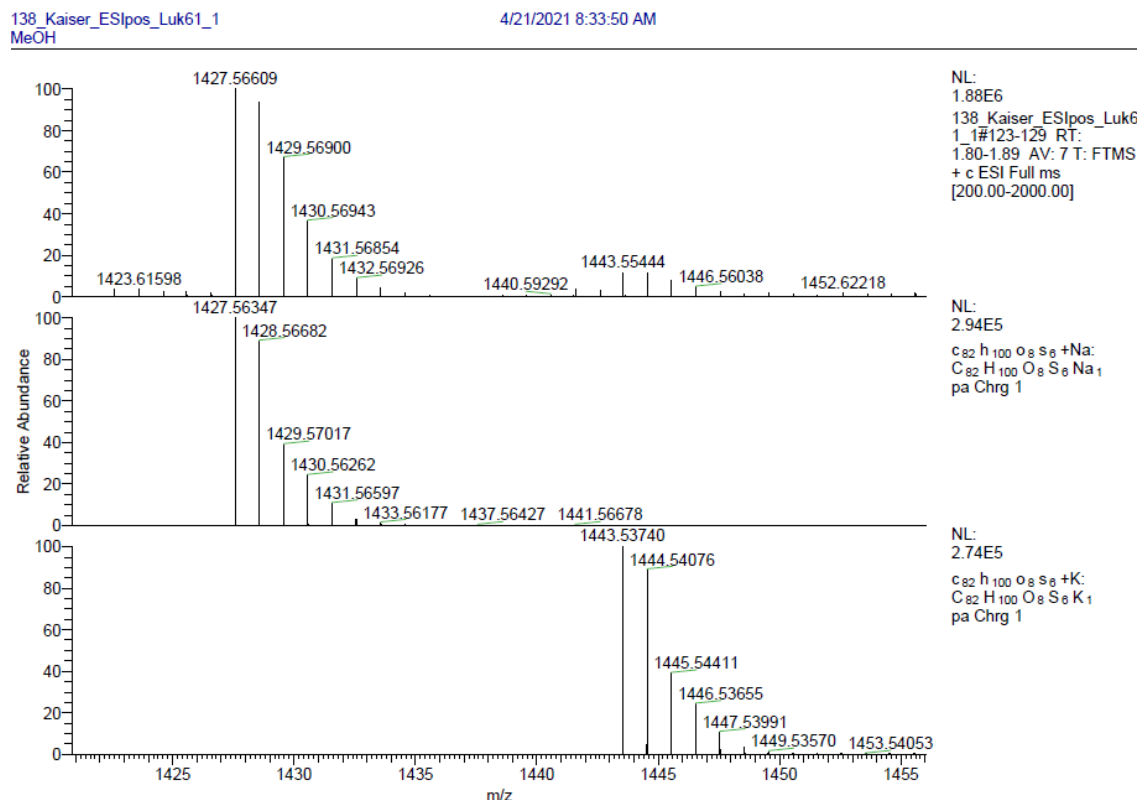


Figure 50. HRMS of compound 18 (ESI⁺) dimer isotopes

2. Fullerene complexation experiments

¹H NMR titration of compound **13** with C₆₀ in toluene-d₈

$$m(\mathbf{13}) = 0.00152 \text{ g}$$

$$m(C_{60}) = 0.00289 \text{ g}$$

$$m(\text{toluene}-d_8) = 1.41035 \text{ g}$$

$$M(\mathbf{13}) = 1063.48 \text{ g/mol}$$

$$M(C_{60}) = 720.64 \text{ g/mol}$$

Number of added eqv.	c(C ₆₀) mol/l	c(13) mol/l	δ (ppm)
0	0.000956	0	3.8316
0.08	0.000956	7.86E-05	3.8359
0.16	0.000956	0.00015	3.8395
0.24	0.000956	0.00023	3.8433
0.38	0.000956	0.00036	3.8472
0.52	0.000956	0.00049	3.8500
0.70	0.000956	0.00067	3.8521
0.97	0.000956	0.00093	3.8570
1.20	0.000956	0.00115	3.8605
1.57	0.000956	0.00150	3.8655
1.87	0.000956	0.00178	3.8692
2.10	0.000956	0.00201	3.8706
2.29	0.000956	0.00219	3.8712
2.45	0.000956	0.00234	3.8714
2.58	0.000956	0.00247	3.8718
2.70	0.000956	0.00258	3.8721

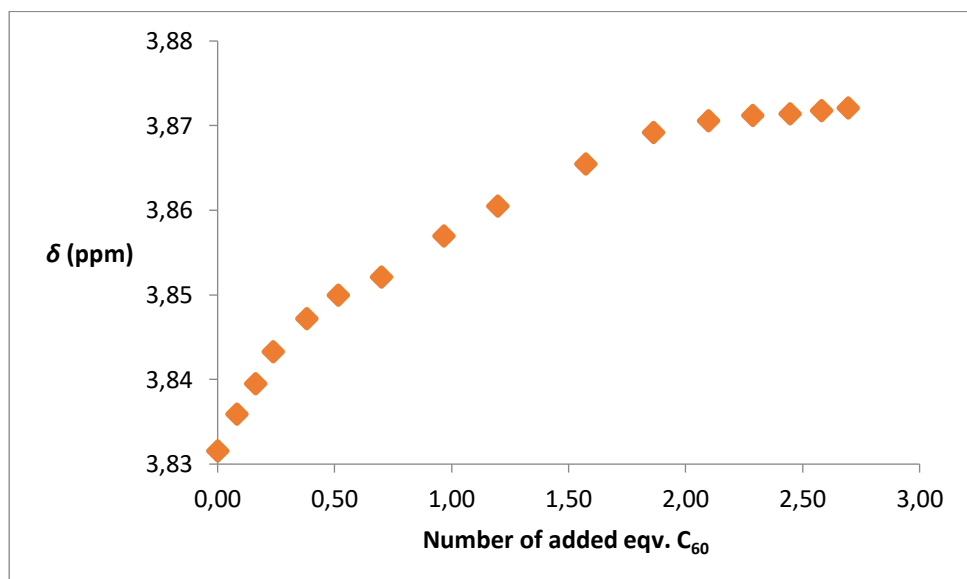


Figure 51. Titration curve for compound **13** - fullerene C₆₀ system. ¹H NMR titration in toluene-d₈, 298 K, 400 MHz.

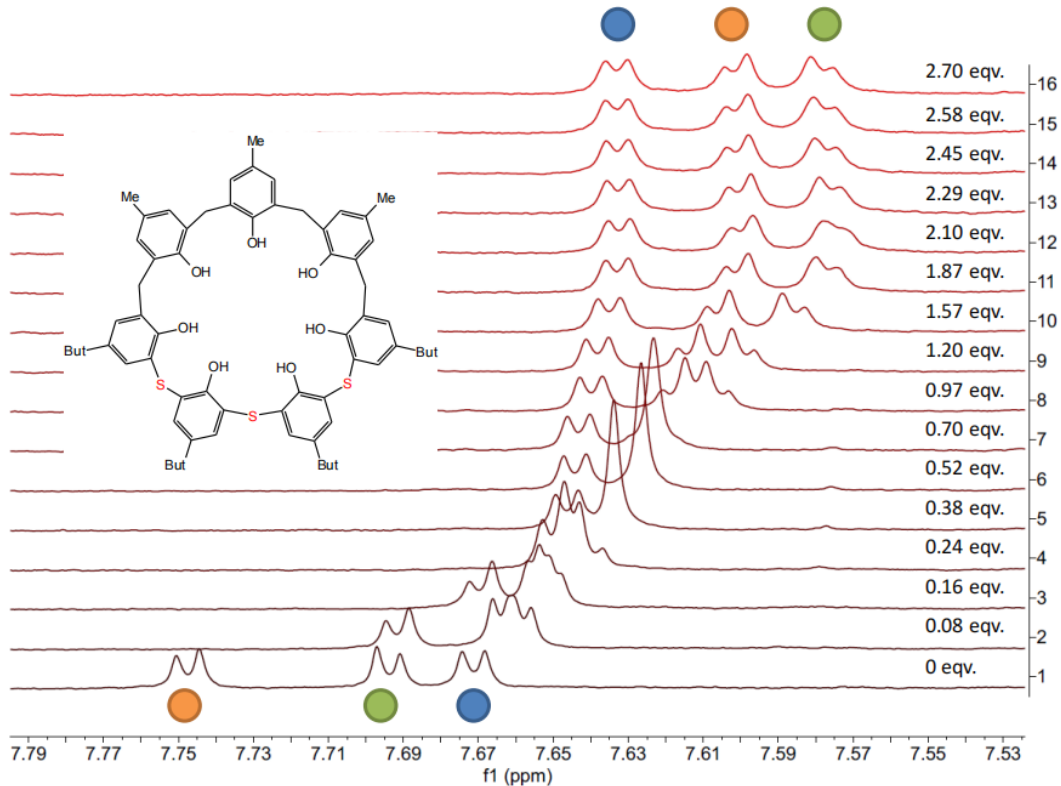


Figure 52. ¹H NMR titration of compound **13** with C_{60} in toluene-*d*₈ (aromatic part of spectrum); 400 MHz, 298 K.

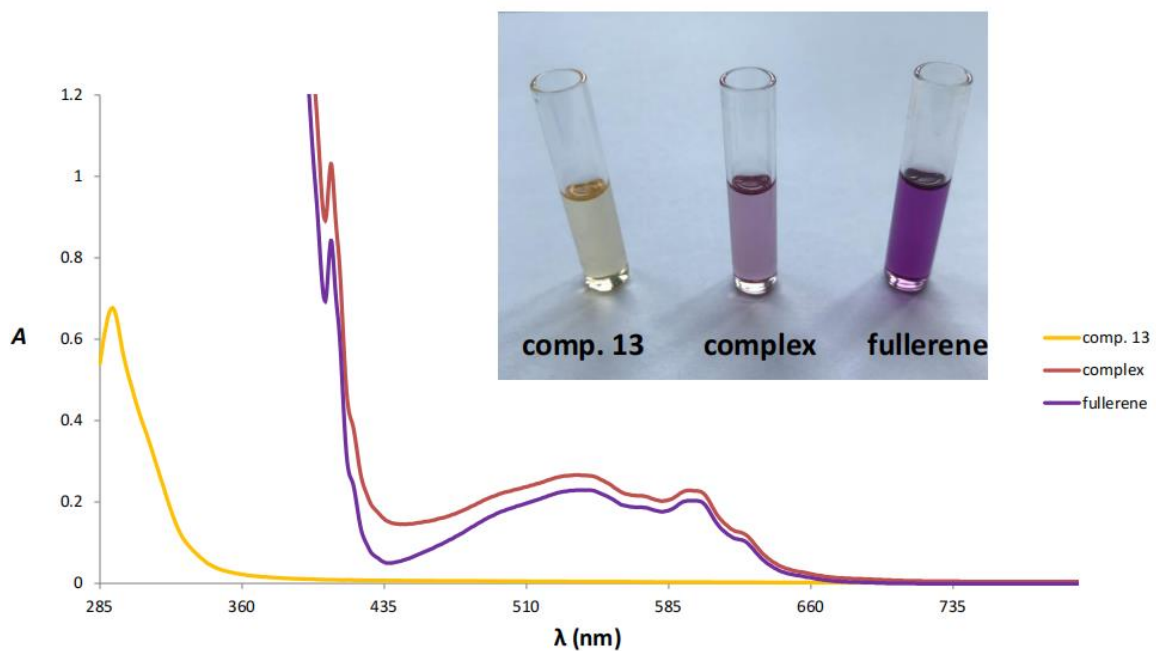


Figure 53. UV-Vis spectra of compound **13**, C_{60} and the corresponding complex.

UV-Vis titration of compound **13** with C₆₀ in toluene

$$m(\mathbf{13}) = 0.00651 \text{ g}$$

$$m(C_{60}) = 0.00198 \text{ g}$$

$$m(\text{toluene}) = 0.93815 \text{ g}$$

$$M(\mathbf{13}) = 1063.48 \text{ g/mol}$$

$$M(C_{60}) = 720.64 \text{ g/mol}$$

Number of added eqv. 13	c(C ₆₀) mol/l	c(13) mol/l	A (UV-Vis) $\lambda = 400 \text{ nm}$
0	0.00254	0	0.789
0.09	0.00254	0.00024	0.822
0.19	0.00254	0.00047	0.834
0.27	0.00254	0.00069	0.853
0.44	0.00254	0.00111	0.876
0.59	0.00254	0.00150	0.899
0.80	0.00254	0.00204	0.927
1.11	0.00254	0.00283	0.965
1.38	0.00254	0.00350	0.998
1.81	0.00254	0.00460	1.050
2.14	0.00254	0.00545	1.088
2.40	0.00254	0.00610	1.119
4.82	0.00254	0.01225	1.301

Cuvettes with pathlengths of 1 mm

$$K = 140 \pm 2 \text{ \%}$$

$$K = 35$$

$$\beta = 4\,900$$

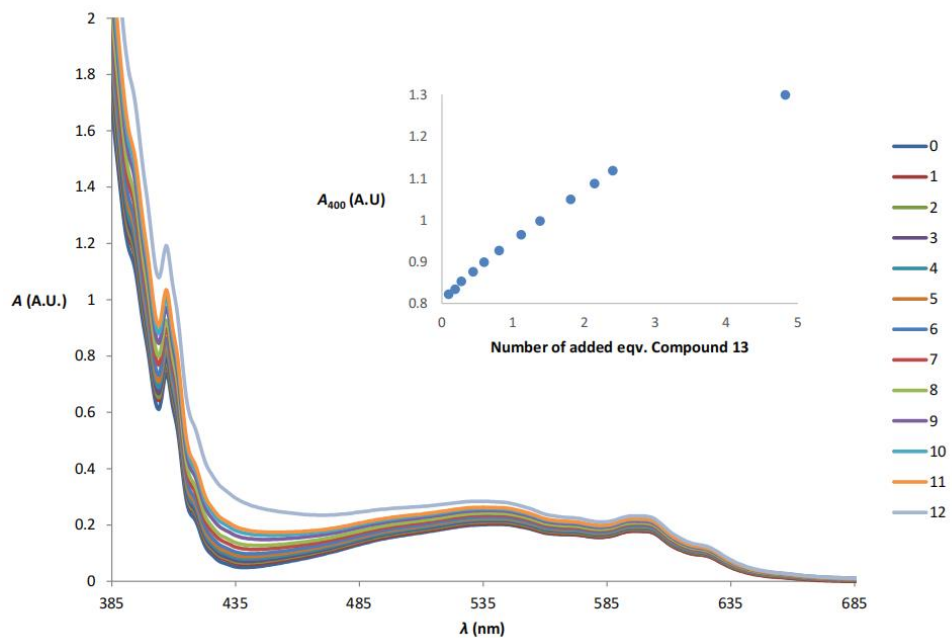


Figure 54. UV-Vis titration of C₆₀ with compound **13** in toluene.

UV-Vis titration of compound **13** with C₇₀ in toluene

$$m(\mathbf{13}) = 0.00253 \text{ g}$$

$$m(C_{70}) = 0.00101 \text{ g}$$

$$m(\text{toluene}) = 0.9392 \text{ g}$$

$$M(\mathbf{13}) = 1063.48 \text{ g/mol}$$

$$M(C_{70}) = 840.75 \text{ g/mol}$$

Number of added eqv. 13	c (C ₇₀) mol/l	c (13) mol/l	A (UV-Vis) $\lambda = 410 \text{ nm}$
0	0.00111	0	1.345
0.08	0.00111	0.00009	1.371
0.17	0.00111	0.00018	1.381
0.24	0.00111	0.00027	1.392
0.39	0.00111	0.00043	1.409
0.53	0.00111	0.00058	1.428
0.72	0.00111	0.00079	1.443
0.99	0.00111	0.00110	1.460
1.23	0.00111	0.00136	1.476
1.61	0.00111	0.00178	1.497
1.91	0.00111	0.00211	1.512
2.10	0.00111	0.00233	1.520
4.29	0.00111	0.00476	1.542

Cuvettes with pathlengths of 1 mm

$$K_{\text{Ass}} = 3100 \pm 5 \%$$

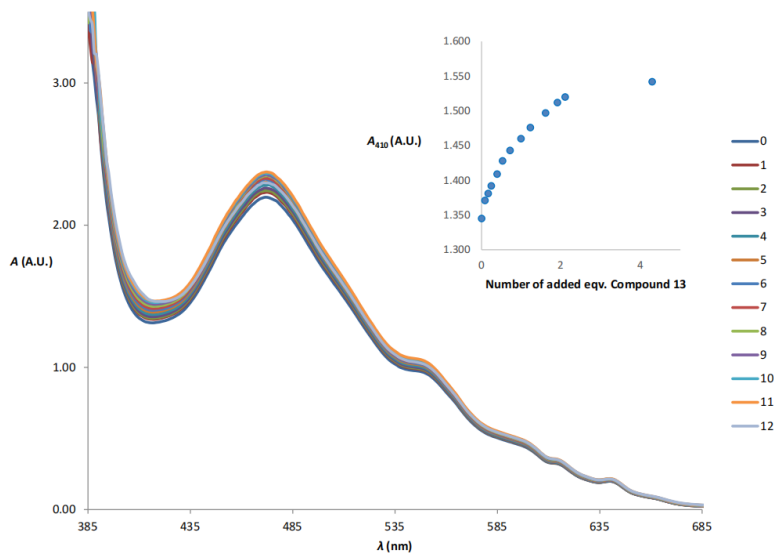


Figure 55. UV-Vis titration of C₇₀ with compound **13** in toluene.

3. Crystallographic data

Crystallographic data for 8

$M = 929.36 \text{ g.mol}^{-1}$, triclinic system, space group $P\bar{1}$, $a = 13.2330(3) \text{ \AA}$, $b = 14.4941(4) \text{ \AA}$, $c = 14.6750(4) \text{ \AA}$, $\alpha = 71.9424(11)^\circ$, $\beta = 82.1907(11)^\circ$, $\gamma = 89.1864(12)^\circ$, $Z = 2$, $V = 2650.05(12) \text{ \AA}^3$, $D_c = 1.165 \text{ g.cm}^{-3}$, $\mu(\text{Cu-K}\alpha) = 1.66 \text{ mm}^{-1}$, crystal dimensions of $0.21 \times 0.11 \times 0.09 \text{ mm}$. Data were collected at 200 (2) K on D8 Venture Photon CMOS diffractometer with Incoatec microfocus sealed tube Cu-K α radiation. The structure was solved by charge flipping methods¹ and anisotropically refined by full matrix least squares on F^2 squared using the CRYSTALS² to final value $R = 0.055$ and $wR = 0.153$ using 9633 independent reflections ($\Theta_{\max} = 68.2^\circ$), 668 parameters and 94 restraints. The hydrogen atoms attached to carbon atoms were placed in calculated positions, refined with weak restraints and then refined with a riding constrains. The hydrogen atoms attached to oxygen atoms were refined with restrained geometry. The disordered functional groups positions were found in difference electron density maps and refined with restrained geometry. The occupancy was constrained to full for each functional group. MCE³ was used for visualization of electron density maps. Diamond 3.0⁴ was used for molecular graphics. The structure was deposited into Cambridge Structural Database under number CCDC 2110419.

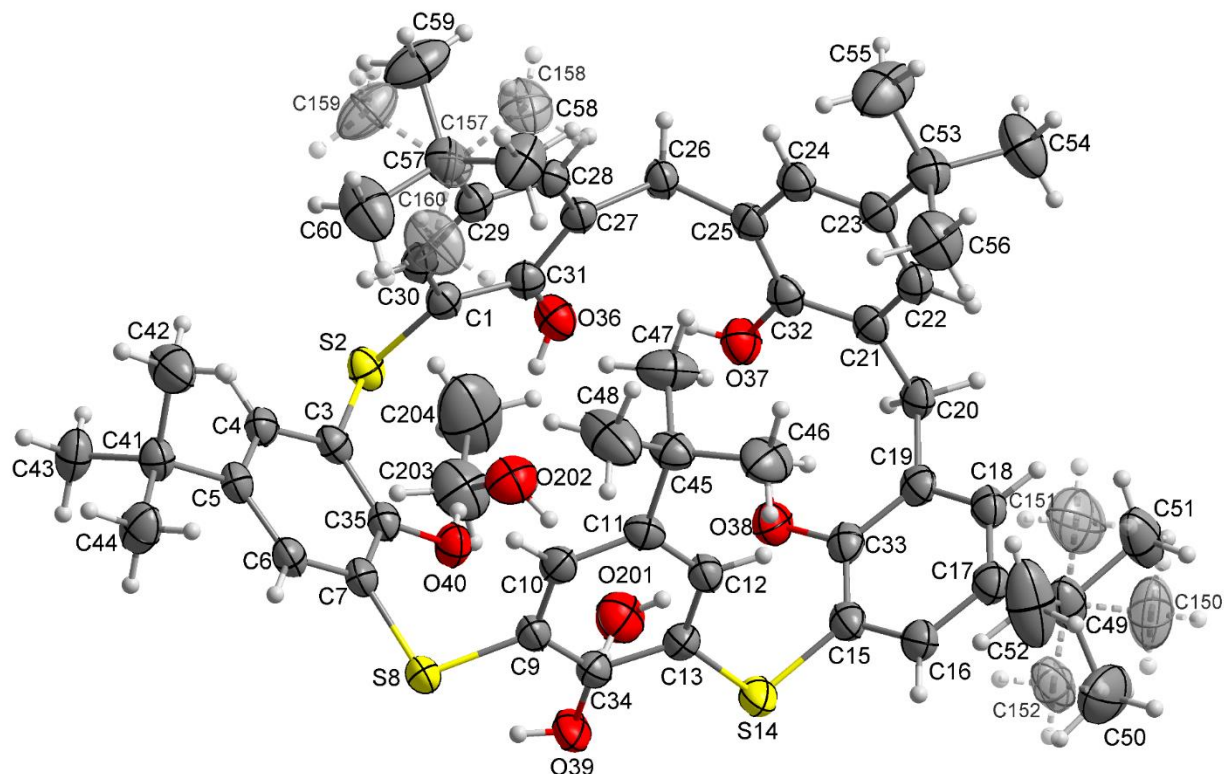
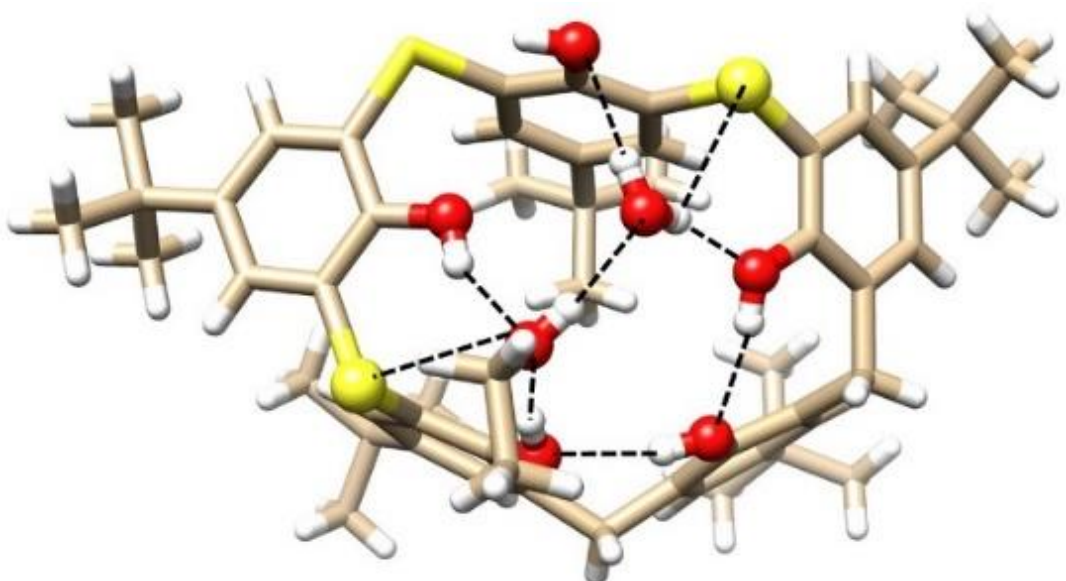


Figure 56. The numbering scheme of compound **8** with ADPs depicted at 50 % probability level.



a)

b)

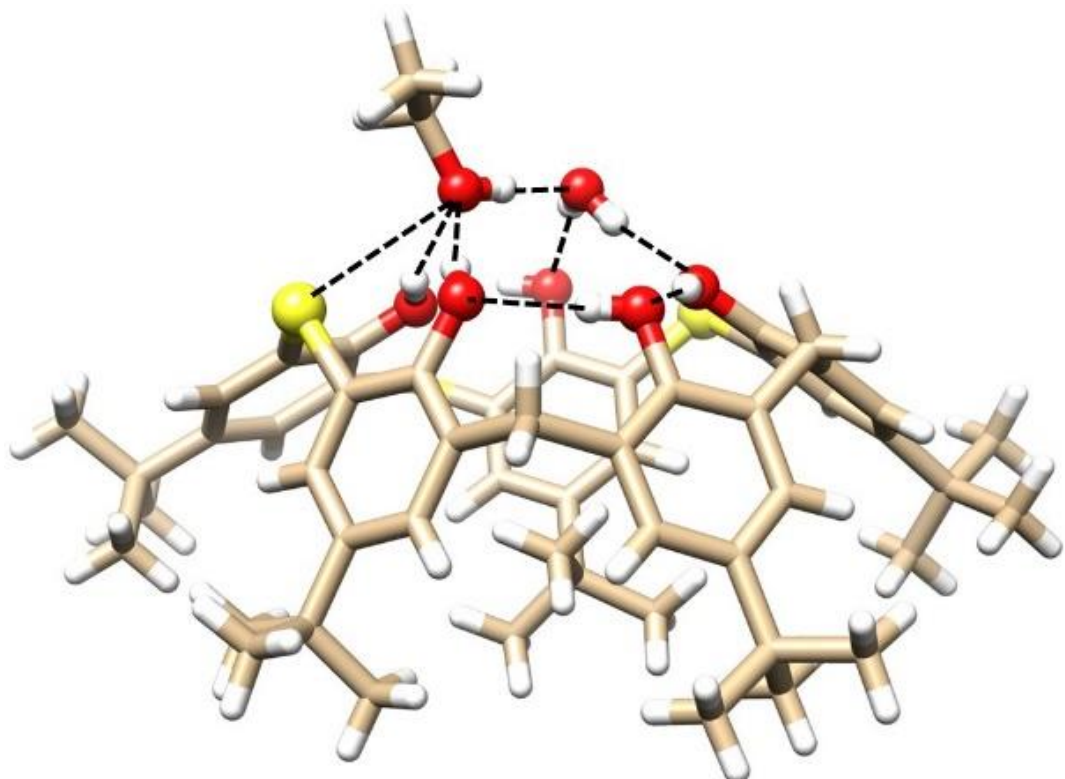


Figure 56a. Single crystal X-ray structures of compound **8**·EtOH·H₂O: (a) top-view showing the array of HBs, (b) side-view (interacting atoms shown as balls for better clarity).

Crystallographic data for 9

$M = 1201.81 \text{ g.mol}^{-1}$, triclinic system, space group $P\bar{1}$, $a = 11.1603(3) \text{ \AA}$, $b = 11.9646(3) \text{ \AA}$, $c = 13.1785(3) \text{ \AA}$, $\alpha = 81.0129(10)^\circ$, $\beta = 70.9839(9)^\circ$, $\gamma = 80.0849(10)^\circ$, $Z = 1$, $V = 1629.33(7) \text{ \AA}^3$, $D_c = 1.225 \text{ g.cm}^{-3}$, $\mu(\text{Cu-K}\alpha) = 2.35 \text{ mm}^{-1}$, crystal dimensions of $0.18 \times 0.15 \times 0.12 \text{ mm}$. Data were collected at 200(2) K on a D8 Venture Photon CMOS diffractometer with Incoatec microfocus sealed tube Cu-K α radiation. The structure was solved by charge flipping methods¹ and anisotropically refined by full matrix least squares on F^2 squared using the CRYSTALS² to final value $R = 0.033$ and $wR = 0.082$ using 5978 independent reflections ($\Theta_{\max} = 68.4^\circ$), 440 parameters and 62 restraints. The hydrogen atoms attached to carbon atoms were placed in calculated positions, refined with weak restraints and then refined with a riding constraints. The hydrogen atoms attached to oxygen atoms were refined with restrained geometry. The disordered bridging atoms were refined with sum of sulfur atom occupancies restrained to 2 and the occupancy of each position constrained to 1. The disordered solvent positions were located in difference electron density maps and refined with restrained geometry. The solvent occupancy was refined with the sum constrained to 1. MCE³ was used for visualization of electron density maps. Diamond 3.0⁴ was used for molecular graphics. The structure was deposited into Cambridge Structural Database under number CCDC 2110418.

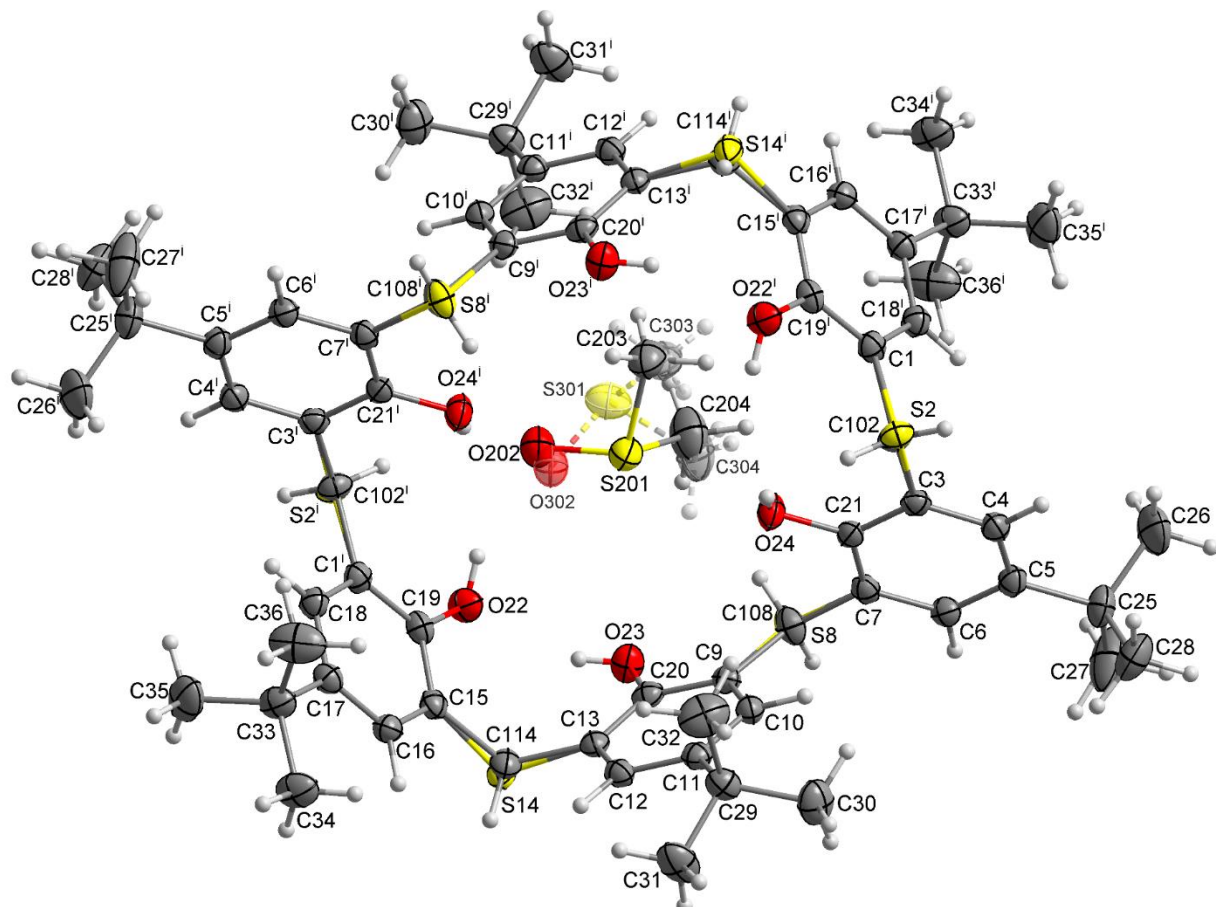


Figure 57. The numbering scheme of compound 9 with ADPs depicted at 50 % probability level. Symmetry code: (i) $1-x, 2-y, 1-z$.

4. References

1. L. Palatinus and G. Chapuis, *J. Appl. Cryst.* 2007, **40**, 786-790.
2. P. W. Betteridge, J. R. Carruthers, R. I. Cooper, K. Prout and D. J. Watkin, *J. Appl. Cryst.* 2003, **36**, 1487.
3. J. Rohlicek and M. Husak, *J. Appl. Cryst.* 2007, **40**, 600.
4. K. Brandenburg, DIAMOND. Crystal Impact GbR, 1999, Bonn, Germany.